

Title: Does phenology explain plant-pollinator interactions at different latitudes? An assessment of its explanatory power in plant-hoverfly networks in French calcareous grasslands

Authors: Natasha de Manincor^{1*}, Nina Hautekeete¹, Yves Piquot¹, Bertrand Schatz², Cédric Vanappelghem³, François Massol^{1,4}

¹Université de Lille, CNRS, UMR 8198 - Evo-Eco-Paleo, 59000 Lille, France

²CEFE, EPHE-PSL, CNRS, University of Montpellier, University of Paul Valéry Montpellier 3, IRD, Montpellier, France

³Conservatoire d'espaces naturels Nord et du Pas-de-Calais, 160 rue Achille Fanien - ZA de la Haye, 62190 LILLERS

⁴Univ. Lille, CNRS, Inserm, CHU Lille, Institut Pasteur de Lille, U1019 - UMR 8204 - CIIL - Center for Infection and Immunity of Lille, F-59000 Lille, France

E-mail addresses and ORCID numbers:

Natasha de Manincor: natasha.de-manincor@univ-lille.fr, 0000-0001-9696-125X

Nina Hautekeete: nina.hautekeete@univ-lille.fr, 0000-0002-6071-5601

Yves Piquot: yves.piquot@univ-lille.fr, 0000-0001-9977-8936

Bertrand Schatz: bertrand.schatz@cefe.cnrs.fr, 0000-0003-0135-8154

Cédric Vanappelghem: cedric.vanappelghem@espaces-naturels.fr

François Massol: francois.massol@univ-lille.fr, 0000-0002-4098-955X

Short title: Phenology and plant-hoverfly interactions

Keywords: Bayesian model, interaction probability, latent block model, latitudinal gradient, mutualistic network, phenology overlap, species abundance, structural equation model.

*Corresponding author information: Natasha de Manincor, e-mail: natasha.de-manincor@univ-lille.fr, phone: +330362268530

26 **Author contributions**

27 NDM and FM conceived the project, formulated and implemented the model. NDM conducted the
28 analysis and prepared the manuscript. FM supervised the analysis and edited the manuscript. NH, YP,
29 CV and BS contributed substantially to all later versions. NDM, NH, YP and BS conducted the fieldwork
30 and provided the data. CV identified the hoverflies.

31 **Data accessibility**

32 The data supporting the results are archived on Zenodo (DOI: 10.5281/zenodo.2542845).

33

Abstract

For plant-pollinator interactions to occur, the flowering of plants and the flying period of pollinators (i.e. their phenologies) have to overlap. Yet, few models make use of this principle to predict interactions and fewer still are able to compare interaction networks of different sizes. Here, we tackled both challenges using Bayesian Structural Equation Models (SEM), incorporating the effect of phenology overlap, in six plant-hoverfly networks. Insect and plant abundances were strong determinants of the number of visits, while phenology overlap alone was not sufficient, but significantly improved model fit. Phenology overlap was a stronger determinant of plant-pollinator interactions in sites where the average overlap was longer and network compartmentalization was weaker, i.e. at higher latitudes. Our approach highlights the advantages of using Bayesian SEMs to compare interaction networks of different sizes along environmental gradients and articulates the various steps needed to do so.

INTRODUCTION

Understanding how phenology determines species interactions is a central question in the case of mutualistic networks. In plant-pollinator networks, phenology shapes their temporal and spatial limits, thus defining the area and the period along the season in which interactions preferably occur (Olesen *et al.* 2011; Ogilvie & Forrest 2017). Since plant and pollinator phenologies are not equally affected by changes in environmental cues, partial or total phenological mismatches can occur as a result of environmental changes such as climate change (Parmesan 2007; Rafferty 2017). Phenological advances indeed increase at higher latitudes, as a response to the acceleration of warming temperature along the same gradient (Post *et al.* 2018), increase phenological mismatch, and have the potential to threaten the synchrony needed for effective pollination (Hutchings *et al.* 2018). Such environmental changes can thus drastically alter pollinator interactions through modified temporal overlap between pollinators and their floral resources leading, in extreme cases, to local extinctions (Memmott *et al.* 2007) and the ensuing absence of the partner species at the location and/or time at which the interaction should have taken place (Willmer 2012; Miller-Struttmann *et al.* 2015; Rafferty *et al.* 2015; Hutchings *et al.* 2018).

Because phenological match is crucial to plant-pollinator interactions, and thus ultimately to pollinators' fitness, pollinators have to adapt to phenological shifts either through interaction with other plant species (Rafferty *et al.* 2015) or through changes of their own phenology (Bartomeus *et al.* 2011). Phenology can then influence dynamical network properties, such as the stability and the coexistence of species, through changes in network topology (Encinas-Viso *et al.* 2012). Moreover, phenology predictably affects network compartmentalization as different phenophases likely correspond to different compartments when networks are considered on an annual scale (Martín González *et al.* 2012).

Despite considerable theoretical advances, there are few models available to predict the probability of interaction in plant-pollinator networks and fewer still able to make comparisons between

networks. Due to their complexity and variation among years (Chacoff *et al.* 2018), most studies of mutualistic networks have focused on predicting and comparing classic network metrics (nestedness, connectance, modularity, etc.) which are all influenced by network size, *i.e.* the number of plant and insect species (Fortuna *et al.* 2010; Staniczenko *et al.* 2013; Poisot & Gravel 2014; Astegiano *et al.* 2015). Moreover, few studies have compared interaction networks along environmental gradients (Devoto *et al.* 2005; Schleuning *et al.* 2012; Sebastián-González *et al.* 2015; Pellissier *et al.* 2018). In order to compare networks of different sizes, a better alternative is to switch from network-derived metrics to the comparison of output of regression models, which can consider multiple factors and latent variables and assume that the sampled data are just part of a larger unobserved dataset (Grace *et al.* 2010). Large datasets allowing relevant comparisons of networks are rare; they require parallel investigations in rich communities of plants and insects to favour interactions between them. Calcareous grasslands are characterized by highly diverse plant communities with a high proportion of entomophilous species (Baude *et al.* 2016), thus they are a convenient model for such studies. Most plant-insect pollinator networks involve bee species (Anthophila), but recent studies have also pointed out the importance of hoverflies (Diptera: Syrphidae), which pollinate a large spectrum of wild flowering species (Klecka *et al.* 2018a) and crops (Jauker & Wolters 2008; Rader *et al.* 2011). They usually behave opportunistically, *i.e.* from being pollen generalists as well as pollen or nectar specialists, only limited by morphological constraints (Iler *et al.* 2013; Klecka *et al.* 2018a; Lucas *et al.* 2018). Indeed, their generalisation could be the result of serial specialized diets, since most pollen retrieved on hoverfly individuals usually comes from a single plant taxon (Lucas *et al.* 2018) and depends on flower availability and phenology (Cowgill *et al.* 1993; Colley & Luna 2000). Moreover, some hoverflies have preferences regarding plant colour, morphology and inflorescence height (Branquart & Hemptinne 2000; Colley & Luna 2000; Lunau 2014; Klecka *et al.* 2018b, a).

Here we study the consequences of environmental gradients on plant-pollinator interactions, focusing on how phenology overlap affects interactions between plants and insects in six calcareous grassland sites distributed along a latitudinal gradient. We obtained plant and insect phenologies, abundances,

and interactions in all sites from April to October 2016. We modelled plant-pollinator interaction networks following a Bayesian Structural Equation Modelling approach (SEM) using latent variables. The comparison of 16 SEM models and the analysis of latent block models (LBM) of sampled networks evinced that phenology overlap is an important determinant of plant-pollinator interactions, but is less informative than species abundances and performs heterogeneously among sites. Our results suggest that the use of SEMs to compare networks of different sizes along an environmental gradient is an innovative approach which can help understand the structure of plant-pollinator networks.

MATERIALS AND METHODS

Study sites

We sampled plant and pollinator species in six areas (Fig. S1) of 1 hectare each in different French regions: two sites in Hauts-de-France (Les Larris de Grouches-Luchuel, thereafter noted LAR, 50°11'22.5"N 2°22'02.9"E and Regional natural reserve Riez de Noeux les Auxi, noted R, 50°14'51.85"N 2°12'05.56"E, in départements Pas-de-Calais and Somme), two sites in Normandie (Château Gaillard – le Bois Dumont, noted CG, 49°14'7.782"N 1°24'16.445"E and les Falaises d'Orival, noted FAL, 49°04'40.08"N 1°33'07.254"E, départements: Eure and Seine Maritime) and two sites in Occitanie (Fourches, noted F, 43°56'07.00"N 3°30'46.1"E and Bois de Fontaret, noted BF, 43°55'17.71"N 3°30'06.06"E, département: Gard). The six sites are included in the European NATURA 2000 network; the four sites in Hauts-de-France and Normandie are managed by the Conservatoire d'espaces naturels of Normandie, Picardie and Nord – Pas-de-Calais and the sites in Occitanie by the CPIE Causses méridionaux. We sampled each site once a month from April to October 2016, except for the site of Riez that was sampled from May to October.

Plant-hoverfly observations and sampling

To collect information at the community level, in each site and at each session we realized: (i) a botanic inventory of the flowering species, recorded their abundances and the total flower covering in the area and (ii) a pollinator sampling using a hand net along a variable transect walk.

Flowering plants were identified at the species level. We recorded the abundances of all flowering species. At first, we estimated the total percentage of surface covered by all flowering species in the selected area. We then estimated the relative abundance of each flowering species. We used Braun-Blanquet coefficients of abundance-dominance to rank flowering species: coefficient **5** = 75-100%, coeff **4** = 50-75%, coeff **3**=25-50%, coeff **2** = 10-25%, coeff **1** = 1-10%, coeff **+** = few individuals less than < 1%, coeff **i** = 1 individual. All inventories were realized by the same surveyors to avoid biases.

Pollinator observations were performed by the same team of 3-5 persons each day. The surveyors walked slowly around any potential attractive resource patch included in the selected 1-hectare area for 4h each day. We split the sampling period into 2 hours in the morning (about 10-12h) and 2 hours in the afternoon (about 14-16h) to cover the daily variability of both pollinator (bees and hoverflies, which are more active in the morning than in the afternoon; D'Amen *et al.* 2013) and flower communities. Sampling took place when we had suitable weather conditions for pollinators (following Westphal *et al.* 2008). We sampled all flower-visiting insects and we recorded observed interactions. All sampled insects were immediately put individually in a killing vial with ethyl acetate and were later prepared and pinned in the laboratory and identified at the species level by expert taxonomists. Even if we collected both bees and hoverflies, in this study we focus on syrphids only. Overall, we sampled for 41 days, equivalent to about 164 hours in the field (all the surveyors collected at the same time). For all analyses described here, we only used the list of visited herbaceous plant species and hoverflies which were found visiting a plant. Despite their rarity, we also considered the interactions between hoverflies and plant species of the Fabaceae family because we did not want to exclude data in the absence of the proof of no interaction, even if hoverflies are known to prefer open flowers (Branquart & Hemptinne 2000). However, we observed in the field that they visited Fabaceae species that were already opened by other insects, *e.g.* by large bee species, such as *Eucera* sp. (De Manincor, personal observation).

Plant – hoverfly networks

For each site, we constructed an interaction network consisting of all pairs of interacting plant and insect species, pooling data from all months. A pair of species (i, j) was connected with intensity v when we recorded v visits of insect species i on plant species j in the site. We calculated the network specialization index, $H2'$ (Blüthgen *et al.* 2006) using the `H2fun` function implemented in the `bipartite` package (Dormann *et al.* 2009; R Core Team 2018). We also calculated the standardized specialization index d' (Blüthgen *et al.* 2006) for each plant and insect species as the ratio of the d -value (Kullback-Leibler divergence between the interactions of the focal species and the interactions predicted by the weight of potential partner species in the overall network) to its corresponding d_{max} -value (maximum d -value theoretically possible given the observed number of interactions in the network). We obtained these values using the `dFUN` function in the `bipartite` package (Dormann *et al.* 2009), but we did not use the d' values provided by this package as they sometimes yielded spurious results based on the computation of the minimal d value (e.g. reporting low d' for species with only one partner in the network).

We calculated the modularity of the network and the associated partition of species into modules using the `cluster_leading_eigen` method for modularity optimization implemented in the `igraph` package (Csardi & Nepusz 2006; Newman 2006). Modularity optimization can help gauge strong, simple divisions of a network in relatively independent sub-networks by looking for densest sub-networks. However, modules are not meant to inform about more subtle groupings among the species, e.g. particular avoidance of interactions between insects of group A and plants of group 1. In order to detect such groups, we implemented latent block models (LBM) using the `BM_poisson` method for Poisson probability distribution implemented in the `blockmodels` package (Leger *et al.* 2015). Blocks are calculated separately for the two groups (insect and plant) based on the number of visits (*i.e.* a weighted network). The algorithm finds the best divisions of insects and plants through fitting one Poisson parameter in each block of the visit matrix, thus essentially maximizing the ICL (Integrated Completed Likelihood; Biernacki *et al.* 2000; Daudin *et al.* 2008). The LBM script is given in

Supplementary Information (Appendix S3). All analyses were performed in R version 3.3.3 (R Core Team 2018).

Plant and hoverfly abundances and phenology overlap

We calculated plant abundance using information about the abundance-dominance recorded in the field following the methodology of Braun-Blanquet presented above. We transformed the coefficients of abundance in percentages (Table S1): we used the mean of the percentage which correspond to each class. We then calculated the relative abundance (A_P) of each flowering plant species as the ratio of the focal species cumulated abundance to total flower abundance during its flowering season. We used the recorded number of visiting hoverflies and their presence (recorded months) along the season to calculate their average abundance during months when they were present (A_H).

We refer to plant phenology as their flowering period and insect phenology as the flying period. We considered only flowering plants which had been visited by pollinators. For the pollinators, we considered only hoverflies which were found in interaction. To build the species phenology tables for both plants and hoverflies, we merged the information provided by two sources of data (field data and the literature): we used the observed phenology of both plants and insects during the field session as the only source of information for plants (plants visited by insects and plants found in the botanic inventory in the site at that date), and we complemented the hoverfly phenology with information provided by the Syrph the Net Database (Speight *et al.* 2016). We then built the phenology overlap (PO) matrix based on the species phenology tables by calculating the number of phenologically active months that are shared by each pair of insect and plant species along the season.

Bayesian Structural Equation Modelling (SEM)

We modelled the hoverfly-plant interaction network using a Bayesian Structural Equation Modelling approach (SEM, Fig. 1) with latent variables linking the number of visits per plant-pollinator dyad to abundance and phenology overlap (PO) data through a first latent table representing probabilities of interactions, another latent table representing the possible interactions between plant and pollinators

(as a realization of the aforementioned interaction probability matrix), and a third latent table yielding the expected number of visits per plant-pollinator dyad (*i.e.* the intensity of interactions).

In this model, we considered that PO had an effect on possible interactions (I_{ij}) and the number of visits (λ_{ij}) – a longer overlap is intuitively expected to drive a higher probability of interaction and a larger number of visits. Interaction probabilities were also assumed to depend on two random effects (plant and insect species identities), to represent heterogeneity of species degrees in the network. We modelled the probability of interaction I_{ij} between insect species i and plant species j (*i.e.* $I_{ij} = 1$ when species i and j can interact) as a Bernoulli random variable of mean μ_{ij} given by:

$$\text{logit}(\mu_{ij}) = \mu_0 + \mu_{PO}PO_{ij} + E_i + E_j$$

where logit is the usual logistic transformation ($\log(x/(1-x))$), μ_0 is the intercept of this relation, μ_{PO} is the coefficient measuring the effect of PO, and E_i and E_j are the random effects associated with insect species i and plant species j respectively.

The number of interactions was assumed to depend on plant and hoverfly abundances, as more abundant species are expected to be more often sampled (and thus more often recorded “in interaction”). The number of visits V_{ij} was modelled as a Poisson random variable to allow for sampling variability, with a conditional mean λ_{ij} (the intensity of visits that can occur) given by:

$$\log(\lambda_{ij}) = \lambda_0 + \lambda_H A_H + \lambda_P A_P + \lambda_{PO} \log(1 + PO)$$

where λ_0 is the intercept of this relation, λ_H is the coefficient measuring the effect of hoverfly abundance A_H , λ_P is that of plant abundance A_P , and λ_{PO} is the coefficient of the effect of PO.

Possible interactions (I_{ij}) and the intensity of visits (λ_{ij}) are multiplied to obtain the unconditional mean number of recorded visits, *i.e.* V_{ij} is then obtained as a Poisson draw of mean $I_{ij} \lambda_{ij}$.

Overall we thus estimated four main parameters: the effect of plant abundance on the intensity of interactions ($A_P \rightarrow \lambda_{ij}$, coefficient λ_P), the effect of insect (hoverflies) abundance on the intensity of

interactions ($A_H \rightarrow \lambda_{ij}, \lambda_H$), the effect of phenology overlap on the intensity of interactions ($PO \rightarrow \lambda_{ij}, \lambda_{PO}$) and the effect of phenology overlap on the probability of interaction ($PO \rightarrow I_{ij}, \mu_{PO}$).

We used the `jags` function (R2jags package), which provides an interface from R to the JAGS library for Bayesian data analysis, to estimate model parameters. JAGS (Plummer 2003) uses a Markov Chain Monte Carlo algorithm to generate samples from the posterior distribution of the parameters. We ran two Markov chains with 10^6 iterations per chain to check for model convergence. The code of the model is given in Supplementary Material (Appendix S1 and S2).

Model and parameter comparison

We estimated the 16 models that included between 0 and 4 of the above-mentioned effects to understand which effects were more likely to play a role in the structuring of the network. The goodness-of-fit of these models were compared using the leave-one-out cross-validation criterion (LOO) calculated using the R package `loo` (Vehtari *et al.* 2017). Models can thus be ranked according to their LOO scores, with the best model being the one with the lowest LOO value. The LOO criterion is analogous to the classic Akaike and Bayesian Information Criteria, but can be applied to Bayesian models without suffering the same instability issues of the Deviance Information Criterion (Vehtari *et al.* 2017). To rank the models, we then calculated the ΔLOO (noted Δ_i) as $\Delta_i = LOO_i - LOO_{min}$ (following Burnham & Anderson 2004), where LOO_{min} is the minimum of the LOO_i values among the 16 models. We used Δ_i to obtain model weights ω_i , following the Akaike weight methodology (Burnham & Anderson 2002):

$$\omega_i = \frac{e^{-\Delta_i/2}}{\sum e^{-\Delta_i/2}}$$

We then summed weights (w_H) over all models that incorporated a given focal parameter to ascertain the plausibility of the effect associated to this parameter. We used this sum to evaluate the null hypothesis (H_0) that a given factor has no effect on the plant-pollinator interactions by comparing the sum of weights to null expectations, based on the fact that each tested effect is incorporated in exactly

half of the tested models. The effect is considered *plausible* when $w_H > 0.5$, *implausible* otherwise, *likely* when $w_H > 0.73$, and *unlikely* when it corresponds to a value of 0.27 or lower, following Massol *et al.* (2007).

RESULTS

Plant-hoverfly networks and phenology overlap

At the end of the field campaign we had collected 1584 hoverflies and recorded 1668 interactions between 76 hoverfly species and 117 plant species overall (Table 1). The number of sampled hoverfly and plant species varied between sites and among regions. In Normandie we generally sampled a higher number of hoverflies than in the other two regions (Table 1). We observed the highest diversity of both plants and hoverflies in Occitanie and the lowest diversity of hoverflies in Hauts-de-France. Despite the high species diversity in Occitanie, the number of interactions recorded in these sites (BF and F) is not the highest recorded in the field (Table 1).

In spite of differences in diversity and the number of interactions, the overall level of specialization (H2 index) did not show a high variation among the 6 networks (range: 0.32 – 0.37). However, we found that the sites in Occitanie (BF and F) had a higher average degree of specialization (d') for both insect (BF 0.63 and F 0.57) and plant species (BF 0.58 and F 0.48). The sites in Occitanie also had a higher modularity (BF 0.51 and F 0.48) than the ones in Normandie (CG 0.34 and FAL 0.23) and Hauts-de-France (LAR 0.37 and R 0.34; Table 1). Given that these statistics only compare 6 sites, none of these assessments can be properly statistically tested, but the importance of the differences among sites is highly suggestive of a difference in average specialization and modularity. We found that plant phenology is generally shorter in all sites than that of hoverflies (Table 1). The phenology overlap was shorter in Occitanie (BF and F) than in the other sites (Table 1).

Illustrations of the block clustering provided by the LBM analysis (Latent Block Model) are shown in Fig. 2 and 3 in the main text and in Fig. S2 to S5 in Supplementary Information. We found different numbers of blocks in plants and hoverflies among sites: the BF site had 2 insect blocks and 2 plant

blocks (Fig. S2); the F site had 4 of both (Fig. 2); the CG and R sites had 3 blocks for the plants and 4 blocks for the insects in (Fig. 3 and S5); the FAL site had 4 plant blocks and 3 insect blocks (Fig. S3); the LAR site had 3 blocks for the plants and 2 for the insects (Fig. S4).

Model ranking and comparison of parameters in each site

For each site we compared the 16 models using the LOO criterion (Table 2, ΔLOO values). We found that models 1, 2 and 4 had consistently better goodness-of-fit than the others. The model incorporating all effects except the effect of phenological overlap on the probability of interaction (Model 4: $\lambda_{ij} \sim A_H + A_P + \text{PO}$, Table 2) was the best model in the sites of CG, FAL and LAR. In the two southern sites (BF and F), we found that the model incorporating all effects except that of phenological overlap on the intensity of visits (Model 1: $\lambda_{ij} \sim A_H + A_P / I_{ij} \sim \text{PO}$, Table 2), was the best one. The model incorporating all effects (Model 0: $\lambda_{ij} \sim A_H + A_P + \text{PO} / I_{ij} \sim \text{PO}$, Table 2) was found as the best one only in the site of R, but was a suitable model ($\Delta\text{LOO} < 4$) in all the other sites (Table 2). We also compared the sum of model weights of the four parameters among sites (Table 2, Evidence ratio). We found that the effect of insect abundance on the intensity of interaction ($A_H \rightarrow \lambda_{ij}$) is always likely (*i.e.* the sum of their weights is always higher than 0.73, Table 2) and of large effect size in all sites (standardised coefficient higher than 1, Fig. 4). Likewise, we found that the effect of plant abundance on the intensity of interaction ($A_P \rightarrow \lambda_{ij}$) was always likely and had large effect size in most part of sites, except in the site of F (ER = 0.59, Table 2; standardised coefficient = 0.67, Fig. 4). The effects of phenological overlap on the probability of interaction ($\text{PO} \rightarrow I_{ij}$) and the intensity of visits ($\text{PO} \rightarrow \lambda_{ij}$), however, had variable plausibility among sites. The effect of phenological overlap on the probability of interaction was *likely* only in half of the sites (Table 2 and Fig. 4). The effect of phenological overlap on the intensity of visits was *not plausible* only in the two southern sites (BF and F) and *plausible* in the other four sites (LAR, R CG and FAL, Table 2 and Fig. 4). In all sites, the standardised coefficients of PO effects were always less than 1, thus suggesting a low effect size of phenology on interaction probability and intensity (Fig. 4).

DISCUSSION

Latitude affects the seasonality, advancing species phenologies at higher latitudes, and thus, can be a limiting factor for the phenological coupling of interacting species (Post *et al.* 2018). In this study we explored the effect of phenology overlap on a large network of species interactions in calcareous grasslands and how this effect could vary along a latitudinal gradient in France using empirical data on six plant-hoverfly networks. We identified plants and insects at the species level to build detailed interaction networks and hence avoid spurious generalisation levels. In order to better understand the determinants of variation in species interactions in space and time, we used the latitudinal gradient to consider variations linked to environmental cues and the entire flowering period to allow for seasonal variation (Valverde *et al.* 2016; Pellissier *et al.* 2018). One of the main problems of comparing networks along gradients is the dependence of networks metrics on network size (Staniczenko *et al.* 2013; Astegiano *et al.* 2015; Tylianakis & Morris 2017). In this study, we employed Bayesian Structural Equation Models (SEM) to link the numbers of visits to abundance and phenology overlap (PO) through latent probabilities of species interaction and expected numbers of visits per plant-pollinator dyad. We tested different models with variable numbers of effects and compared them in each site. SEM is an emergent approach increasingly used to investigate complex networks of relationship in ecological studies (Grace *et al.* 2010; Eisenhauer *et al.* 2015; Fan *et al.* 2016; Theodorou *et al.* 2017).

We found that in all sites the most important effect affecting pollinator visits was insect abundance (Table 2). Likewise we found that plant abundance was also a very important effect in most part of sites, except in the site of F (Table 2). Species abundance often explain the linkage level in pollination network studies (Olesen *et al.* 2008; Bartomeus *et al.* 2016; Chacoff *et al.* 2018; Pellissier *et al.* 2018) but it is often associated with the length of the phenology to better assess the general properties of the interaction network (Vázquez *et al.* 2009; Olito & Fox 2015). In accordance with this verbal prediction, we indeed found that the best models incorporated the effect of PO on either the probability or the intensity of interactions (Table 2). Phenology overlap generally cannot predict the

probability of interaction on its own (Encinas-Viso *et al.* 2012; CaraDonna *et al.* 2017). Our findings do agree with this general predicament since no site favoured a model that only incorporated PO effects and because these effects always display lower effect sizes than the other variables. In our model, the effect of PO on the probability of interaction and the expected number of visits also vary along the latitudinal gradient (Fig. 4).

In general, we observed that southern sites (BF and F) showed shorter plant phenology and phenology overlap (PO) than the other four sites (Table 1). In these sites, plant species richness is higher and fewer visits were sampled, probably because the presence of specialist species with short phenophases may increase the number of forbidden or undetected links (Olesen *et al.* 2011; Martín González *et al.* 2012). Conversely, in sites where plant phenology is longer, PO is longer too, as observed in Normandie and Hauts-de-France (CG, FAL, LAR and R, Table 1). Moreover, when plant richness and specialization are lower, a higher number of visits can be observed (Table 1) because generalist species could interact without constraints. Indeed, in Normandie and Hauts-de-France we found that the effect of phenology overlap on the intensity of visits was always likely ($PO \rightarrow \lambda_{ij}$, Table 2) and we observed higher numbers of interactions in the first two/three blocks of insects and plants which also corresponded to blocks with longer PO (Fig. 3, S3, S4 and S5). A higher phenological overlap is expected to drive a higher probability of interactions and a larger number of visits (Olesen *et al.* 2011). In Occitanie, we did not find any effect of PO on the number of visits because the more densely visited blocks do not correspond to those with longer phenology overlap. Plant phenology can therefore drive the probability and the intensity of interactions in networks in which plant phenology is shorter, thus suggesting that syrphid flies may undergo selection for behavioural flexibility in order to maintain synchrony with their foraging resources (Iler *et al.* 2013; Ogilvie & Forrest 2017).

We also found that modularity decreased along the latitudinal gradient, with richer sites (BF and F) displaying higher modularity (as in Sebastián-González *et al.* 2015). In the two southern sites, higher modularity could be related to shorter phenologies and higher proportions of non-overlapping sets of

species, which induce some form of temporal short-term specialisation (Lucas *et al.* 2018). However, modularity also seems to be influenced by species abundances and degrees (Schleuning *et al.* 2014), and is expected to increase with link specificity (Morente-López *et al.* 2018). Indeed, in these sites, species blocks match species degrees (Fig. 2 and S2), with generalist and specialist species forming separate blocks among both plants and insects (Martín González *et al.* 2012). With lower modularity and more generalist species, we expect a stronger relationship between phenology and the intensity of interactions because interactions are less influenced by insect preferences and more by seasonal rhythm and flower availability (Dormann *et al.* 2017). Thus, different phenophases might correspond to different compartments (Martín González *et al.* 2012; Morente-López *et al.* 2018), as observed in CG, FAL, LAR and R where higher overlap corresponded to higher numbers of observed visits. Although phenology improved model fit (Table 2), its effect size was modest (Fig. 4), which suggests that other types of data such as traits and phylogenies might help predict specific interactions. In our study, we did not consider competition among studied insect species or with other group of insects, such as bees which were present in all sites. Different types of pollinators with different abundances could have context-dependent effects on network topology (Valverde *et al.* 2016).

To conclude, plant phenology here drives the duration of the phenology overlap between plant and insects, which in turn influences either the probability of interaction or the expected number of visits, as well as network compartmentalization. Longer phenologies correspond to less constrained interactions (lower modularity), shorter phenologies to more constrained interactions (higher modularity), which in turn restrict the number of visits. Phenology overlap alone was not sufficient to explain interactions, as suggested elsewhere (CaraDonna *et al.* 2017). Plant and insect abundances played a substantial role to explain the number of visits (as in (Chacoff *et al.* 2018)) since abundances may affect partner choice (Trøjelsgaard *et al.* 2015). Our results, and the ability of the method used here to compare different effects on interaction patterns, suggest that the use of Bayesian SEM to compare networks of different sizes is a valuable tool which can help understand plant-pollinator networks (Eisenhauer *et al.* 2015). The use of latent variables can help predict the probability of

interaction and the expected number of visits while avoiding circularity – the introduction of plant and insect specific random effects played the role of an implicit “degree” effect. Our results demonstrate the importance of considering differences in plant and insect phenologies to better predict their interactions in pollination networks at different latitudes. The use of morphological traits (*e.g.* tongue length, inter-tegular distance, ...) together with species richness and phylogenies, on top of variables already used, might improve the modelling of interactions and could help better understand some forbidden or missing links in richer communities or considering other pollinators (*e.g.* wild bees).

ACKNOWLEDGEMENTS

Financial support was provided by the ANR ARSENIC project (grant no. 14-CE02-0012), the Region Nord-Pas-de-Calais and the CNRS. We also thank Martin Speight for insect identification, Clément Mayozer for informatic support and all the students who took part in the field campaign. This work is a contribution to the CPER research project CLIMIBIO. The authors thank the French Ministère de l'Enseignement Supérieur et de la Recherche, the Hauts-de-France Region and the European Funds for Regional Economical Development for their financial support.

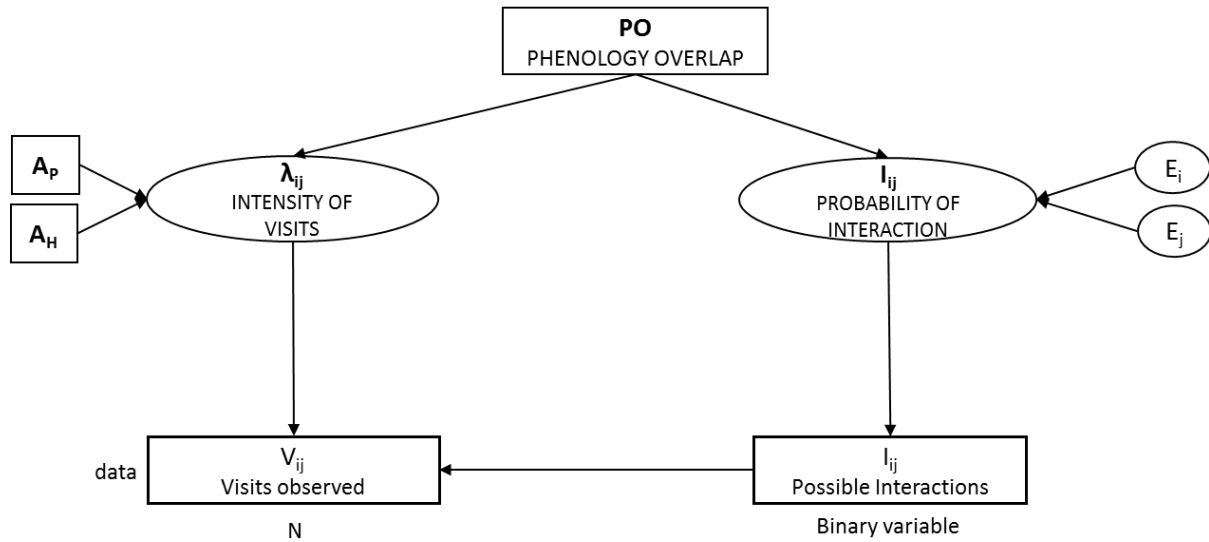
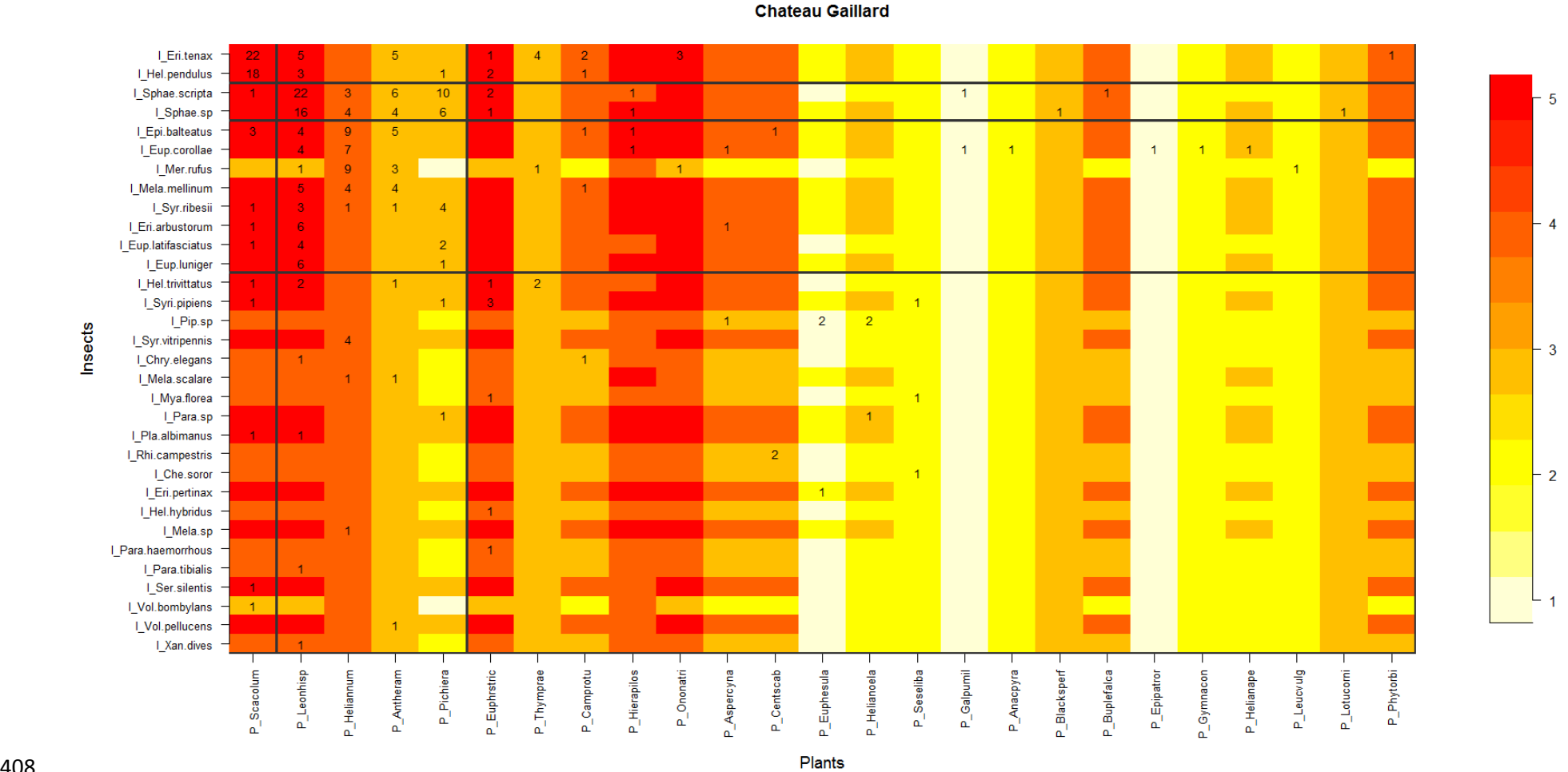


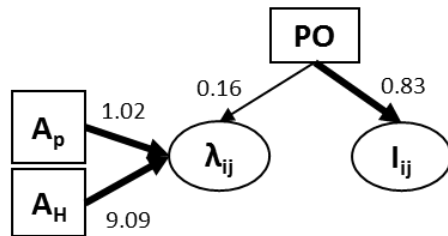
Figure 1. Summary diagram of the SEM model. We estimated 4 effects: the effect of plant abundance ($A_P \rightarrow \lambda_{ij}$, coefficient λ_P), the effect of insect (hoverflies) abundance on the intensity of visits ($A_H \rightarrow \lambda_{ij}$, λ_H), the effect of phenology overlap on the intensity of visits ($PO \rightarrow \lambda_{ij}$, λ_{PO}) and the effect of phenology overlap on the probability of interaction ($PO \rightarrow I_{ij}$, μ_{PO}). The phenology overlap (PO) is the number of phenologically active months that are shared by each pair of insect and plant species along the season. The intensity of visits (λ_{ij}) and the probability of interaction are latent variables in the model. Effect-i and effect-p are random effects calculated by the model which represent the insect and plant degrees. The I_{ij} (Possible interactions) is a binary variable and the V_{ij} (visits observed) follow a Poisson distribution with an expected value given when the probability of interaction is predicted as “true”. Rectangles represent observed variables while ovals represent unobserved influences.

Figure 3. Block clustering provided by LBM in the site of Chateau Gaillard (CG, Normandie) overlaid on a heatmap of species phenology overlap. Insect species are displayed in rows and plant species in columns, following their degree (number of partners). The blocks of insects and the blocks of plants are separated by solid black lines. Colours correspond to the number of months that are shared by each pair of plant and insect species (PO, phenology overlap), with higher PO corresponding to darker colours. Numbers are the number of visits observed in the field for a given plant-insect pair.

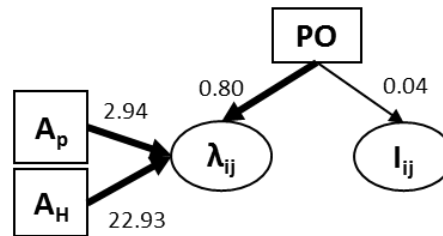


409 Figure 4. Summary diagram of the best models in all sites. The thickness of the arrows is scaled to Akaike weights (thin ER < 0.73; thick ER > 0.73, cf. Table 2).
 410 Standardised coefficients of the model average (computed based on the Akaike weighted model average) are reported next to the arrows. PO is the phenology
 411 overlap, I_{ij} is the probability of interaction, λ_{ij} is the intensity of visits, A_H and A_p are the hoverflies and plant abundances respectively.

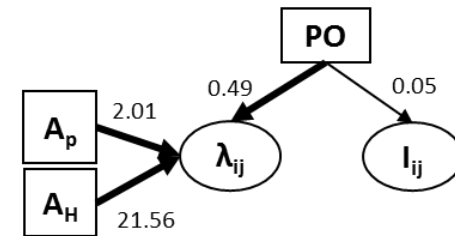
BOIS DE FONTARET



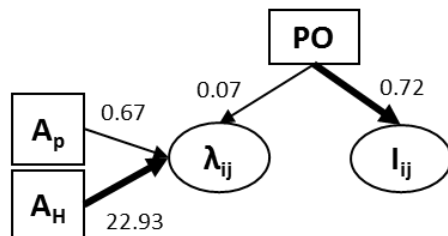
CHÂTEAU GAILLARD



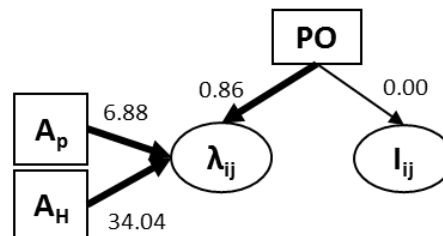
LARRIS



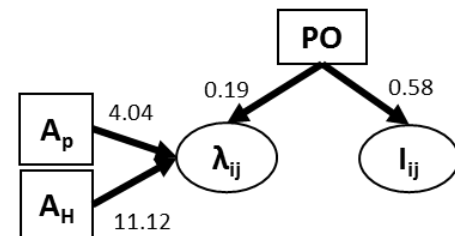
FOURCHES



FALAISES



RIEZ



414 Table 1. Summary table of results obtained in each site (Bois de Fontaret [BF] and Fourches [F] in Occitanie, Château Gaillard [CG] and Falaises [FAL] in
415 Normandie, Larris [LAR] and Riez [R] in Hauts-de-France). H_2' and d' indices refer to specialization indices described by Blüthgen *et al.* (2006) and
416 implemented in the R package *bipartite* (Dormann *et al.* 2009). The modularity score was obtained using the *leading-eigenvector* method
417 described by Newman (2006) and implemented in the *igraph* package (Csardi & Nepusz 2006). LBM refers to latent block modelling as implemented in the
418 R package *blockmodels* (Leger *et al.* 2015).

419

Site	Region	Collected data				Specialization index			Species phenology			Modularity analysis	LBM	
		Sampled insects	Insect species	Plant species	Recorded Interactions	H_2' index	d' Insects (average + sd)	d' Plants (average + sd)	Insect (average + sd)	Plant (average + sd)	Phenology overlap (PO) (average + sd)	modularity score	blocks I	blocks P
BF	Occitanie	197	40	43	198	0.37	0.63 ± 0.17	0.58 ± 0.17	5.25 ± 1.51	2.14 ± 1.04	1.77 ± 1.03	0.53	2	2
F	Occitanie	223	36	49	286	0.33	0.57 ± 0.18	0.48 ± 0.19	5.61 ± 1.54	2.08 ± 1.13	1.78 ± 1.14	0.48	4	4
CG	Normandie	295	32	25	297	0.34	0.40 ± 0.21	0.47 ± 0.18	6.03 ± 1.00	3.28 ± 1.24	3.02 ± 1.17	0.34	4	3
FAL	Normandie	363	34	30	374	0.32	0.40 ± 0.18	0.41 ± 0.18	6.06 ± 1.13	3.57 ± 1.59	3.23 ± 1.51	0.23	3	4
LAR	Hauts-de-France	220	24	33	220	0.36	0.48 ± 0.19	0.45 ± 0.15	6.38 ± 0.82	3.18 ± 1.38	2.99 ± 1.36	0.37	2	3
R	Hauts-de-France	286	22	29	293	0.32	0.39 ± 0.16	0.40 ± 0.16	5.55 ± 0.74	3.38 ± 1.47	3.11 ± 1.45	0.34	4	3
Total		1584	76	117	1668									

420

Table 2. (i) Comparison of SEM models using the leave-one-out cross-validation criterion (LOO); (ii) evidence ratios (ER) of model effects in each site. (i) Models are ranked depending on the number of parameters used (from 0 to 4). The best models are the ones with $\Delta\text{LOO}=0$ (underlined and bold values). The other suitable models are the ones with $\Delta\text{LOO} < 4$ (underlined and italic values). λ_{ij} is the intensity of visits, I_{ij} is the probability of interaction, A_H is the insect abundance, A_P is the plant abundance and PO is the phenology overlap. (ii) We compared 4 model effects: $\text{PO} \rightarrow I_{ij}$, effect of the phenology overlap on the probability of interaction; $\text{PO} \rightarrow \lambda_{ij}$, effect of the phenology overlap on the intensity of visits; $A_H \rightarrow \lambda_{ij}$ and $A_P \rightarrow \lambda_{ij}$ effects of the hoverflies and plant abundances on the intensity of interaction. The ER limits for unlikelihood is 0.27, plausibility 0.5 and likelihood 0.73. Underlined and bold values represent the likely hypothesis only.

			Sites					
			BF	F	CG	FAL	LAR	R
Model	Nb of parameters	$\Delta\text{LOO values}$						
0 $\lambda_{ij} \sim A_H + A_P + \text{PO} / I_{ij} \sim \text{PO}$	4	<u>2.98</u>	<u>2.04</u>	<u>3.54</u>	<u>2.54</u>	<u>2.86</u>	0.00	
1 $\lambda_{ij} \sim A_H + A_P / I_{ij} \sim \text{PO}$	3	0.00	0.00	36.75	64.04	10.37	<u>2.90</u>	
2 $\lambda_{ij} \sim A_P + \text{PO} / I_{ij} \sim \text{PO}$	3	8.66	78.23	106.46	184.02	44.60	17.00	
3 $\lambda_{ij} \sim A_H + \text{PO} / I_{ij} \sim \text{PO}$	3	6.63	<u>1.71</u>	8.09	73.62	11.24	11.42	
4 $\lambda_{ij} \sim A_H + A_P + \text{PO}$	3	<u>2.86</u>	8.06	0.00	0.00	0.00	<u>2.24</u>	
5 $\lambda_{ij} \sim \text{PO} / I_{ij} \sim \text{PO}$	2	14.69	73.20	109.85	223.86	55.67	23.09	
6 $\lambda_{ij} \sim A_H / I_{ij} \sim \text{PO}$	2	<u>1.45</u>	<u>1.31</u>	33.53	119.04	27.23	19.76	
7 $\lambda_{ij} \sim A_P / I_{ij} \sim \text{PO}$	2	9.84	72.16	156.61	256.04	47.99	21.53	
8 $\lambda_{ij} \sim A_H + \text{PO}$	2	11.49	8.18	5.25	71.97	10.28	13.80	
9 $\lambda_{ij} \sim A_P + \text{PO}$	2	10.71	88.67	103.46	182.14	44.36	17.94	
10 $\lambda_{ij} \sim A_H + A_P$	2	24.36	14.04	36.10	66.82	10.51	4.26	
11 $I_{ij} \sim \text{PO}$	1	11.78	68.52	154.26	272.98	64.12	32.39	
12 $\lambda_{ij} \sim \text{PO}$	1	19.99	86.20	108.46	219.66	54.64	25.73	
13 $\lambda_{ij} \sim A_H$	1	25.58	14.41	36.12	123.30	28.27	22.78	
14 $\lambda_{ij} \sim A_P$	1	32.99	87.70	157.74	256.39	48.82	22.87	
15 -	0	34.39	83.89	155.68	274.80	64.78	33.52	
Model effects		Evidence ratio (ER)						
$\text{PO} \rightarrow I_{ij}$		0.88	0.98	0.15	0.22	0.20	0.74	
$\text{PO} \rightarrow \lambda_{ij}$		0.26	0.35	1.00	1.00	0.99	0.79	
$A_H \rightarrow \lambda_{ij}$		0.99	1.00	1.00	1.00	1.00	1.00	
$A_P \rightarrow \lambda_{ij}$		0.74	0.59	0.93	1.00	0.99	1.00	

433 **Supporting Information**

434 The following Supporting Information is available for this article:

435 Appendix S1. Model code.

436 Appendix S2. Model script for the 16 models.

437 Appendix S3. Script modularity and latent block model analysis (LBM).

438 Figure S1. Sites location in France.

439 Figure S2. Block clustering provided by LBM in the site of Bois de Fontaret (BF, Occitanie), overlaid on
440 a heatmap of species phenology overlap.

441 Figure S3. Block clustering provided by LBM in the site of Falaises (FAL, Normandie), overlaid on a
442 heatmap of species phenology overlap.

443 Figure S4. Block clustering provided by LBM in the site of Larris (LAR, Hauts-de-France), overlaid on a
444 heatmap of species phenology overlap.

445 Figure S5. Block clustering provided by LBM in the site of Riez (R, Hauts-de-France), overlaid on a
446 heatmap of species phenology overlap.

447 Table S1. Table of transformed plant abundances.

448

REFERENCES

- Astegiano, J., Massol, F., Vidal, M.M., Cheptou, P.O. & Guimarães, P.R. (2015). The robustness of plant-pollinator assemblages: Linking plant interaction patterns and sensitivity to pollinator loss. *PLoS One*, 10, e0117243.
- Bartomeus, I., Ascher, J.S., Wagner, D., Danforth, B.N., Colla, S., Kornbluth, S., *et al.* (2011). Climate-associated phenological advances in bee pollinators and bee-pollinated plants. *Proc. Natl. Acad. Sci. U. S. A.*, 108, 20645–9.
- Bartomeus, I., Gravel, D., Tylianakis, J.M., Aizen, M.A., Dickie, I.A. & Bernard-Verdier, M. (2016). A common framework for identifying linkage rules across different types of interactions. *Funct. Ecol.*, 30, 1894–1903.
- Baude, M., Kunin, W.E., Boatman, N.D., Conyers, S., Davies, N., Gillespie, M.A.K., *et al.* (2016). Historical nectar assessment reveals the fall and rise of floral resources in Britain. *Nature*, 530, 85–88.
- Biernacki, C., Celeux, G. & Govaert, G. (2000). Assessing a mixture model for clustering with integrated completed likelihood. *IEEE Trans. Pattern Anal. Mach. Intell.*, 22, 719–725.
- Blüthgen, N., Menzel, F. & Blüthgen, N. (2006). Measuring specialization in species interaction networks. *BMC Ecol.*, 6, 9.
- Branquart, E. & Hemptinne, J. (2000). Selectivity in the exploitation of floral resources by hoverflies (Diptera: Syrphinae). *Ecography (Cop.)*, 23, 732–742.
- Burnham, K.P. & Anderson, D.R. (2002). *Model Selection and Multimodel Inference A Practical Information-Theoretic Approach*. 2nd Editio. Springer-Verlag, New York.
- Burnham, K.P. & Anderson, D.R. (2004). Multimodel inference: Understanding AIC and BIC in model selection. *Sociol. Methods Res.*, 33, 261–304.
- CaraDonna, P.J., Petry, W.K., Brennan, R.M., Cunningham, J.L., Bronstein, J.L., Waser, N.M., *et al.* (2017). Interaction rewiring and the rapid turnover of plant – pollinator networks. *Ecol. Lett.*, 20, 385–394.
- Chacoff, N.P., Resasco, J. & Vázquez, D.P. (2018). Interaction frequency, network position, and the temporal persistence of interactions in a plant–pollinator network. *Ecology*, 99, 21–28.
- Colley, M.R. & Luna, J.M. (2000). Relative attractiveness of potential beneficial insectary plants to aphidophagous hoverflies (Diptera: Syrphidae). *Environ. Entomol.*, 29, 1054–1059.
- Cowgill, S.E., Wratten, S.D. & Sotherton, N.W. (1993). The selective use of floral resources by the hoverfly *Episyrphus balteatus* (Diptera: Syrphidae) on farmland. *Ann. Appl. Biol.*, 122, 223–231.
- Csardi, G. & Nepusz, T. (2006). The igraph software package for complex network research. *InterJournal, Complex Sy*, 1695.
- D’Amen, M., Birtele, D., Zapponi, L. & Hardersen, S. (2013). Patterns in diurnal co-occurrence in an assemblage of hoverflies (Diptera: Syrphidae). *Eur. J. Entomol.*, 110, 649–656.
- Daudin, J.J., Picard, F. & Robin, S. (2008). A mixture model for random graphs. *Stat. Comput.*, 18, 173–183.
- Devoto, M., Medan, D. & Montaldo, N.H. (2005). Patterns of interaction between plants and pollinators along an environmental gradient. *Oikos*, 109, 461–472.

489 Dormann, C.F., Fründ, J., Blüthgen, N. & Gruber, B. (2009). Indices, graphs and null models: analyzing
490 bipartite ecological networks. *Open Ecol. J.*, 2, 7–24.

491 Dormann, C.F., Fründ, J. & Schaefer, H.M. (2017). Identifying causes of patterns in ecological
492 networks: opportunities and limitations. *Annu. Rev. Ecol. Evol. Syst.*, 48, 12–20.

493 Eisenhauer, N., Bowker, M.A., Grace, J.B. & Powell, J.R. (2015). From patterns to causal
494 understanding: Structural equation modeling (SEM) in soil ecology. *Pedobiologia (Jena)*, 58, 65–
495 72.

496 Encinas-Viso, F., Revilla, T.A. & Etienne, R.S. (2012). Phenology drives mutualistic network structure
497 and diversity. *Ecol. Lett.*, 15, 198–208.

498 Fan, Y., Chen, J., Shirkey, G., John, R., Wu, S.R., Park, H., *et al.* (2016). Applications of structural
499 equation modeling (SEM) in ecological studies: an updated review. *Ecol. Process.*, 5, 5–19.

500 Fortuna, M.A., Stouffer, D.B., Olesen, J.M., Jordano, P., Mouillot, D., Krasnov, B.R., *et al.* (2010).
501 Nestedness versus modularity in ecological networks: Two sides of the same coin? *J. Anim.*
502 *Ecol.*, 79, 811–817.

503 Grace, J.B., Anderson, T.M., Olff, H. & Scheiner, S.M. (2010). On the specification of structural
504 equation models for ecological systems. *Ecol. Monogr.*, 80, 67–87.

505 Hutchings, M.J., Robbirt, K.M., Roberts, D.L. & Davy, A.J. (2018). Vulnerability of a specialized
506 pollination mechanism to climate change revealed by a 356-year analysis, 498–509.

507 Iler, A., Inouye, D., Høye, T., Miller-Rushing, A., Burkle, L. & Johnston, E. (2013). Maintenance of
508 temporal synchrony between syrphid flies and floral resources despite differential phenological
509 responses to climate. *Glob. Chang. Biol.*, 19, 2348–2359.

510 Jauker, F. & Wolters, V. (2008). Hover flies are efficient pollinators of oilseed rape. *Oecologia*, 156,
511 819–823.

512 Klecka, J., Biella, P. & Klecka, J. (2018a). Flower visitation by hoverflies (Diptera : Syrphidae) in a
513 temperate plant-pollinator network. *PeerJPreprints*, 19, 780–785.

514 Klecka, J., Hadrava, J. & Koloušková, P. (2018b). Vertical stratification of plant–pollinator interactions
515 in a temperate grassland. *PeerJ*, 6, e4998.

516 Leger, J.B., Daudin, J.J. & Vacher, C. (2015). Clustering methods differ in their ability to detect
517 patterns in ecological networks. *Methods Ecol. Evol.*, 6, 474–481.

518 Lucas, A., Bodger, O., Brosi, B.J., Ford, C.R., Forman, D.W., Greig, C., *et al.* (2018). Generalisation and
519 specialisation in hoverfly (Syrphidae) grassland pollen transport networks revealed by DNA
520 metabarcoding. *J. Anim. Ecol.*, 87, 1008–1021.

521 Lunau, K. (2014). Visual ecology of flies with particular reference to colour vision and colour
522 preferences. *J. Comp. Physiol. A Neuroethol. Sensory, Neural, Behav. Physiol.*, 200, 497–512.

523 Martín González, A.M., Allesina, S., Rodrigo, A. & Bosch, J. (2012). Drivers of compartmentalization in
524 a Mediterranean pollination network. *Oikos*, 121, 2001–2013.

525 Massol, F., David, P., Gerdeaux, D. & Jarne, P. (2007). The influence of trophic status and large-scale
526 climatic change on the structure of fish communities in Perialpine lakes. *J. Anim. Ecol.*, 76, 538–
527 551.

528 Memmott, J., Craze, P.G., Waser, N.M. & Price, M. V. (2007). Global warming and the disruption of

529 plant-pollinator interactions. *Ecol. Lett.*, 10, 710–717.

530 Miller-Struttman, N.E., Geib, J.C., Franklin, J.D., Kevan, P.G., Holdo, R.M., Ebert-may, D., *et al.*
531 (2015). Functional mismatch in a bumble bee pollination mutualism under climate change.
532 *Science*, 349, 1541–4.

533 Morente-López, J., Lara-Romero, C., Ornos, C. & Iriondo, J.M. (2018). Phenology drives species
534 interactions and modularity in a plant - flower visitor network. *Sci. Rep.*, 8, 9386.

535 Newman, M.E.J. (2006). Finding community structure in networks using the eigenvectors of matrices.
536 *Phys. Rev. E - Stat. Nonlinear, Soft Matter Phys.*, 74, 036104.

537 Ogilvie, J.E. & Forrest, J.R. (2017). Interactions between bee foraging and floral resource phenology
538 shape bee populations and communities. *Curr. Opin. Insect Sci.*, 21, 75–82.

539 Olesen, J.M., Bascompte, J., Dupont, Y.L., Elberling, H., Rasmussen, C. & Jordano, P. (2011). Missing
540 and forbidden links in mutualistic networks. *Proc. R. Soc. B Biol. Sci.*, 278, 725–732.

541 Olesen, J.M., Bascompte, J., Elberling, H. & Jordano, P. (2008). Temporal dynamics in a pollination
542 network. *Ecology*, 89, 1573–1582.

543 Olito, C. & Fox, J.W. (2015). Species traits and abundances predict metrics of plant-pollinator network
544 structure, but not pairwise interactions. *Oikos*, 124, 428–436.

545 Parmesan, C. (2007). Influences of species, latitudes and methodologies on estimates of phenological
546 response to global warming. *Glob. Chang. Biol.*, 13, 1860–1872.

547 Pellissier, L., Albouy, C., Bascompte, J., Farwig, N., Graham, C., Loreau, M., *et al.* (2018). Comparing
548 species interaction networks along environmental gradients. *Biol. Rev.*, 93, 785–800.

549 Plummer, M. (2003). JAGS: a program for analysis of Bayesian graphical models using Gibbs sampling.

550 Poisot, T. & Gravel, D. (2014). When is an ecological network complex? Connectance drives degree
551 distribution and emerging network properties. *PeerJ*, 2, e251.

552 Post, E., Steinman, B.A. & Mann, M.E. (2018). Acceleration of phenological advance and warming
553 with latitude over the past century. *Sci. Rep.*, 8, 3927.

554 R Core Team. (2018). R: A language and environment for statistical computing. R Foundation for
555 Statistical Computing, Vienna, Austria. URL <https://www.R-project.org/>.

556 Rader, R., Edwards, W., Westcott, D.A., Cunningham, S.A. & Howlett, B.G. (2011). Pollen transport
557 differs among bees and flies in a human-modified landscape. *Divers. Distrib.*, 17, 519–529.

558 Rafferty, N.E. (2017). Effects of global change on insect pollinators: multiple drivers lead to novel
559 communities. *Curr. Opin. Insect Sci.*

560 Rafferty, N.E., CaraDonna, P.J. & Bronstein, J.L. (2015). Phenological shifts and the fate of
561 mutualisms. *Oikos*, 124, 14–21.

562 Schleuning, M., Fru, J., Klein, A., Abrahamczyk, S., Albrecht, M., Andersson, G.K.S., *et al.* (2012).
563 Report Specialization of Mutualistic Interaction Networks Decreases toward Tropical Latitudes,
564 1925–1931.

565 Schleuning, M., Ingmann, L., Strauß, R., Fritz, S.A., Dalsgaard, B., Matthias Dehling, D., *et al.* (2014).
566 Ecological, historical and evolutionary determinants of modularity in weighted seed-dispersal
567 networks. *Ecol. Lett.*, 17, 454–463.

568 Sebastián-González, E., Dalsgaard, B., Sandel, B. & Guimarães, P.R. (2015). Macroecological trends in
569 nestedness and modularity of seed-dispersal networks: Human impact matters. *Glob. Ecol.*
570 *Biogeogr.*, 24, 293–303.

571 Speight, M.C.D., Castella, E., Sarthou, J.-P. & Vanappelghem, C. (2016). StN 2016. In: Syrph the Net on
572 CD, Issue 11. Speight, M.C.D., Castella, E., Sarthou, J.-P. & Vanappelghem, C. (Eds.) Syrph the
573 Net Publications, Dublin.

574 Staniczenko, P.P.A., Kopp, J.C. & Allesina, S. (2013). The ghost of nestedness in ecological networks.
575 *Nat. Commun.*, 4, 1391–1396.

576 Theodorou, P., Albig, K., Radzevičiūtė, R., Settele, J., Schweiger, O., Murray, T.E., *et al.* (2017). The
577 structure of flower visitor networks in relation to pollination across an agricultural to urban
578 gradient. *Funct. Ecol.*, 31, 838–847.

579 Trøjelsgaard, K., Jordano, P., Carstensen, D.W. & Olesen, J.M. (2015). Geographical variation in
580 mutualistic networks: Similarity, turnover and partner fidelity. *Proc. R. Soc. B Biol. Sci.*, 282,
581 20142925.

582 Tylianakis, J.M. & Morris, R.J. (2017). Ecological networks across environmental gradients. *Annu. Rev.*
583 *Ecol. Evol. Syst.*, 48, 25–48.

584 Valverde, J., Gómez, J.M. & Perfectti, F. (2016). The temporal dimension in individual-based plant
585 pollination networks. *Oikos*, 125, 468–479.

586 Vázquez, D.P., Chacoff, N.P. & Cagnolo, L. (2009). Evaluating multiple determinants of the structure
587 of plant-animal mutualistic networks. *Ecology*, 90, 2039–2046.

588 Vehtari, A., Gelman, A. & Gabry, J. (2017). Practical Bayesian model evaluation using leave-one-out
589 cross-validation and WAIC. *Stat. Comput.*, 27, 1413–1432.

590 Westphal, C., Bommarco, R., Carré, G., Lamborn, E., Morison, M., Petanidou, T., *et al.* (2008).
591 Measuring bee diversity in different European habitats and biogeographic regions. *Ecol.*
592 *Monogr.*, 78, 653–671.

593 Willmer, P. (2012). Ecology: Pollinator-plant synchrony tested by climate change. *Curr. Biol.*, 22,
594 R131–R132.

595

Supplementary Information

Does phenology explain plant-pollinator interactions at different latitudes? An assessment of its explanatory power in plant-hoverfly networks in French calcareous grasslands

N. de Manincor^{1*}, N. Hautekeete¹, Y. Piquot¹, B. Schatz², C. Vanappelghem³, F. Massol^{1,4}

¹ Université de Lille, CNRS, UMR 8198 - Evo-Eco-Paleo, 59000 Lille, France

² CEFE, EPHE-PSL, CNRS, University of Montpellier, University of Paul Valéry Montpellier 3, IRD, Montpellier, France

³ Conservatoire d'espaces naturels Nord et du Pas-de-Calais, 160 rue Achille Fanien - ZA de la Haye, 62190 LILLERS

⁴ Univ. Lille, CNRS, Inserm, CHU Lille, Institut Pasteur de Lille, U1019 - UMR 8204 - CIIL - Center for Infection and Immunity of Lille, F-59000 Lille, France

Natasha de Manincor ORCID: 0000-0001-9696-125X

Nina Hautekeete ORCID: 0000-0002-6071-5601

Yves Piquot ORCID: 0000-0001-9977-8936

Bertrand Schatz ORCID: 0000-0003-0135-8154

François Massol ORCID: 0000-0002-4098-955X

*Corresponding author

E-mail addresses: natasha.de-manincor@univ-lille.fr, francois.massol@univ-lille.fr,
nina.hautekeete@univ-lille.fr, yves.piquot@univ-lille.fr, Bertrand.SCHATZ@cefe.cnrs.fr,
cedric.vanappelghem@espaces-naturels.fr

619 **Appendix S1: Model Code**

620 The model code (in JAGS language) given in this supplementary material refers to the “model Z0” which
 621 considers all four parameters (model effects, Table 2 in the main text). Overall, we estimated 16
 622 models that included between 0 and 4 of the above-mentioned effects. To create the code for these
 623 other models, parameters should be removed following the order in the Tab. 2. The four parameters
 624 tested in the model are: (i) alpha: effect of the phenology overlap (cooc) on the probability of
 625 interaction; (ii) epsilon: effect of the phenology overlap on the intensity of visits; (iii) gamma: effect of
 626 the insect abundances (ab_I) on the intensity of visits; and (iv) delta: effect of the plant abundances
 627 (ab_P) on the intensity of visits.

```

628
629 model
630 {
631   for( i in 1 : dim1 ) {
632     for( p in 1 : dim2 ) {
633       inter[i , p] ~ dbern(mu[i , p])
634       logit(mu[i , p]) <- beta + alpha*cooc[i , p] + effet_I[i] + effet_P[p]
635       lambda[i,p] <- exp(theta[i,p])
636       theta[i,p] <- theta0 + gamma*ab_I[i] + delta*ab_P[p] + epsilon*log(1+cooc[i,p])
637       visit[i,p] ~ dpois( inter[i,p]*lambda[i,p] )
638       loglik[i,p] <- log(ifelse(visit[i,p]==0,1-mu[i,p]+mu[i , p]*dpois(visit[i,p],lambda[i,p]),mu[i ,
639 p]*dpois(visit[i,p],lambda[i,p])))
640     }
641   }
642
643   for( i in 1 : dim1 ) {
644     effet_I[i] ~ dnorm( 0.0,tau_I)

```

```

645     }
646
647     for( p in 1 : dim2 ) {
648         effet_P[p] ~ dnorm( 0.0,tau_P)
649     }
650
651     tau_I ~ dexp( 10)
652     tau_P ~ dexp( 10)
653     alpha ~ dnorm(0,0.01)
654     beta ~ dnorm(0,0.01)
655     theta0 ~ dnorm(0,0.01)
656     gamma ~ dnorm(0,0.01)
657     delta ~ dnorm(0,0.01)
658     epsilon ~ dnorm(0,0.01)
659 }
660

```

661 **Appendix 2: Model script for the 16 models – LOO values**

662 The following generic script was applied to all the study sites using all 16 models. The script is separated
663 in three blocks which communicate among them: the script options, the model definitions and the
664 execution (model inference). We defined three options to set (i) the name of the directory (-d), (ii) the
665 site (-s) and (iii) the type of model (-m).

666 We used, as an example, the information for the site of Bois de Fontaret (BF).

667 Exemple: Rscript (name) "script-SEMLOO_generique.R" "-d o-BFs-2016" "-s BFs"

668 In order to calculate the standardised coefficients for each parameters used, at the end of the third
669 block, we added the functions to get the parameter values for each site and each model.

670 ##### BLOCK 1 – SCRIPT OPTION #####

671 library(optparse)

672 option_list = list(

673 make_option(c("-d", "--dir"), type="character", default=NULL, help="directory",

674 metavar="character"),

675 make_option(c("-s", "--site"), type="character", default=NULL, help="site name",

676 metavar="character"),

677 make_option(c("-m", "--modele"), type="character", default="all", help="modele name",

678 metavar="character"))

679 opt_parser = OptionParser(option_list=option_list);

680 opt = parse_args(opt_parser);

681 site<-opt\$site

682 dossier<-opt\$dir

683 ##### Librairies #####

684 library(bipartite)

685 library(vegan)

686 library(igraph)


```

687 library(magrittr)
688 library(dummies)
689 library(MuMIn)
690 library(rjags)
691 library(boot)
692 library(R2jags)
693 library(coda)
694 library(lattice)
695 library(ggplot2)
696 library(loo)
697 library(matrixStats)
698 ##### Function to record the LOO values #####
699 write_values<-function(x, f, app)
700 {
701     write.table(x, append=app, file=f, sep="\t", row.names=T, col.names=T, quote=F)
702 }
703 ##### BLOCK 2 – MODEL FUNCTIONS #####
704 #Model function and model initialization: one function for each model from model Z15, with 0
705 parameters, to Z00 with all the parameters#
706 ### MODEL Z015
707 mZ015<-function(){
708     init.funZ015 <-function(){
709         list("tau_I" = rexp(1,10), "tau_P" = rexp(1,10), "beta" = rnorm(1,0,1), "theta0" =
710 rnorm(1,0,1), "effet_I"=rnorm(dim1,0,1),"effet_P"=rnorm(dim2,0,1), "inter"=inter0)
711     }

```

```

712     mod.Z015<-jags(inits=init.funZ015,model.file = "modelZ015_code.txt",data =
713     list("visit","dim1","dim2"),parameters.to.save =
714     c("mu","effet_I","effet_P","tau_I","tau_P","beta","theta0", "loglik"),n.chains = 1, n.iter=1000000,
715     n.burnin = 250000, n.thin = 250)
716     mod.Z015.mcmc<-as.mcmc(mod.Z015)
717     mZ015<-mod.Z015$BUGSoutput$sims.list
718     mZ015.deviance<-mZ015$deviance
719     mZ015.loglik<-mZ015$loglik
720     dimSEM<-dim(mZ015.loglik)[1]
721     list.mZ015<-sapply(1:dimSEM,function(x) matrix(mZ015.loglik[x,,],nrow=dim1*dim2))
722     list.tmZ015<-(t(list.mZ015))
723     mZ015.loo<-loo(list.tmZ015)
724     loo_file<-paste(dossier, "/", site, "_Z015_loo.txt", sep="")
725     write_values("mZ015", app=F, loo_file)
726     mZ015_loo_pointwise<-mZ015.loo$pointwise
727     mZ015_loo_pareto_k<-mZ015.loo$pareto_k
728     mZ015.loo$pareto_k<-NULL
729     mZ015.loo$pointwise<-NULL
730     write_values(as.matrix(mZ015.loo), app=T, loo_file)
731     save.image(paste(dossier, "/", site, "_Z015.RData", sep=""))
732 }
733 ### MODEL Z014
734 mZ014<-function(){
735     init.funZ014 <-function(){
736         list("tau_I" = rexp(1,10), "tau_P" = rexp(1,10), "beta" = rnorm(1,0,1), "delta" = rnorm(1,0,1),
737         "theta0" = rnorm(1,0,1), "effet_I"=rnorm(dim1,0,1),"effet_P"=rnorm(dim2,0,1), "inter"=inter0)

```

```

738     }

739     mod.Z014<-jags(inits=init.funZ014,model.file = "modelZ014_code.txt",data =
740     list("visit","ab_P","dim1","dim2"),parameters.to.save =
741     c("mu","effet_I","effet_P","tau_I","tau_P","delta","beta","theta0","loglik"),n.chains = 1,
742     n.iter=1000000, n.burnin = 250000, n.thin = 250)

743     mod.Z014.mcmc<-as.mcmc(mod.Z014)
744     mZ014<-mod.Z014$BUGSoutput$sims.list
745     mZ014.deviance<-mZ014$deviance
746     mZ014.loglik<-mZ014$loglik
747     dimSEM<-dim(mZ014.loglik)[1]
748     list.mZ014<-sapply(1:dimSEM,function(x) matrix(mZ014.loglik[x,,],nrow=dim1*dim2))
749     list.tmZ014<-(t(list.mZ014))
750     mZ014.loo<-loo(list.tmZ014)
751     mZ014.loo
752     loo_file<-paste(dossier, "/", site, "_Z014_loo.txt", sep="")
753     write_values("mZ014", app=T, loo_file)
754     mZ014_loo_pointwise<-mZ014.loo$pointwise
755     mZ014_loo_pareto_k<-mZ014.loo$pareto_k
756     mZ014.loo$pareto_k<-NULL
757     mZ014.loo$pointwise<-NULL
758     write_values(as.matrix(mZ014.loo), app=T, loo_file)
759     save.image(paste(dossier, "/", site, "_Z014.RData", sep=""))
760 }

761 ### MODEL Z013
762 mZ013<-function(){
763     init.funZ013 <-function(){

```

```

764     list("tau_I" = rexp(1,10), "tau_P" = rexp(1,10), "beta" = rnorm(1,0,1), "gamma" =
765     rnorm(1,0,1), "theta0" = rnorm(1,0,1), "effet_I"=rnorm(dim1,0,1),"effet_P"=rnorm(dim2,0,1),
766     "inter"=inter0)
767   }
768   mod.Z013<-jags(inits=init.funZ013,model.file = "modelZ013_code.txt",data =
769   list("visit","ab_I","dim1","dim2"),parameters.to.save =
770   c("mu","effet_I","effet_P","tau_I","tau_P","gamma","beta","theta0","loglik"),n.chains = 1,
771   n.iter=1000000, n.burnin = 250000, n.thin = 250)
772   mod.Z013.mcmc<-as.mcmc(mod.Z013)
773   mZ013<-mod.Z013$BUGSoutput$sims.list
774   mZ013.deviance<-mZ013$deviance
775   mZ013.loglik<-mZ013$loglik
776   dimSEM<-dim(mZ013.loglik)[1]
777   list.mZ013<-sapply(1:dimSEM,function(x) matrix(mZ013.loglik[x,,],nrow=dim1*dim2))
778   list.tmZ013<-(t(list.mZ013))
779   mZ013.loo<-loo(list.tmZ013)
780   mZ013.loo
781   loo_file<-paste(dossier, "/", site, "_Z013_loo.txt", sep="")
782   write_values("mZ013", app=T, loo_file)
783   mZ013_loo_pointwise<-mZ013.loo$pointwise
784   mZ013_loo_pareto_k<-mZ013.loo$pareto_k
785   mZ013.loo$pareto_k<-NULL
786   mZ013.loo$pointwise<-NULL
787   write_values(as.matrix(mZ013.loo), app=T, loo_file)
788   save.image(paste(dossier, "/", site, "_Z013.RData", sep=""))
789 }

```

```

790   ### MODEL Z012
791   mZ012<-function(){
792       init.funZ012 <-function(){
793           list("tau_I" = rexp(1,10), "tau_P" = rexp(1,10), "beta" = rnorm(1,0,1), "theta0" =
794   rnorm(1,0,1), "epsilon" = rnorm(1,0,1), "effet_I"=rnorm(dim1,0,1),"effet_P"=rnorm(dim2,0,1),
795   "inter"=inter0)
796       }
797       mod.Z012<<-jags(inits=init.funZ012,model.file = "modelZ012_code.txt",data =
798   list("cooc","visit","dim1","dim2"),parameters.to.save =
799   c("mu","effet_I","effet_P","tau_I","tau_P","beta","theta0","epsilon","loglik"),n.chains = 1,
800   n.iter=1000000, n.burnin = 250000, n.thin = 250)
801       mod.Z012.mcmc<-as.mcmc(mod.Z012)
802       mZ012<-mod.Z012$BUGSoutput$sims.list
803       mZ012.deviance<-mZ012$deviance
804       mZ012.loglik<-mZ012$loglik
805       dimSEM<-dim(mZ012.loglik)[1]
806       list.mZ012<-sapply(1:dimSEM,function(x) matrix(mZ012.loglik[x,,],nrow=dim1*dim2))
807       list.tmZ012<-(t(list.mZ012))
808       mZ012.loo<-loo(list.tmZ012)
809       mZ012.loo
810       loo_file<-paste(dossier, "/", site, "_Z012_loo.txt", sep="")
811       write_values("mZ012", app=T, loo_file)
812       mZ012_loo_pointwise<-mZ012.loo$pointwise
813       mZ012_loo_pareto_k<-mZ012.loo$pareto_k
814       mZ012.loo$pareto_k<-NULL
815       mZ012.loo$pointwise<-NULL

```

```

816     write_values(as.matrix(mZ012.loo), app=T, loo_file)
817     save.image(paste(dossier, "/", site, "_Z012.RData", sep=""))
818 }
819 ### MODEL Z011
820 mZ011<-function(){
821     init.funZ011 <-function(){
822         list("tau_I" = rexp(1,10), "tau_P" = rexp(1,10), "alpha" = 0.1,"beta" = rnorm(1,0,1), "theta0"
823 = rnorm(1,0,1), "effet_I"=rnorm(dim1,0,1),"effet_P"=rnorm(dim2,0,1), "inter"=inter0)
824     }
825     mod.Z011<-jags(inits=init.funZ011,model.file = "modelZ011_code.txt",data =
826 list("cooc","visit","dim1","dim2"),parameters.to.save =
827 c("mu","effet_I","effet_P","tau_I","tau_P","alpha","beta","theta0","loglik"),n.chains = 1,
828 n.iter=1000000, n.burnin = 250000, n.thin = 250)
829     mod.Z011.mcmc<-as.mcmc(mod.Z011)
830     mZ011<-mod.Z011$BUGSoutput$sims.list
831     mZ011.deviance<-mZ011$deviance
832     mZ011.loglik<-mZ011$loglik
833     dimSEM<-dim(mZ011.loglik)[1]
834     list.mZ011<-sapply(1:dimSEM,function(x) matrix(mZ011.loglik[x,,],nrow=dim1*dim2))
835     list.tmZ011<-(t(list.mZ011))
836     mZ011.loo<-loo(list.tmZ011)
837     mZ011.loo
838     loo_file<-paste(dossier, "/", site, "_Z011_loo.txt", sep="")
839     write_values("mZ011", app=T, loo_file)
840     mZ011_loo_pointwise<-mZ011.loo$pointwise
841     mZ011_loo_pareto_k<-mZ011.loo$pareto_k

```

```

842         mZ011.loo$pareto_k<-NULL
843         mZ011.loo$pointwise<-NULL
844         write_values(as.matrix(mZ011.loo), app=T, loo_file)
845         save.image(paste(dossier, "/", site, "_Z011.RData", sep=""))
846     }
847     ### MODEL Z010
848     mZ010<-function(){
849         init.funZ010 <-function(){
850             list("tau_I" = rexp(1,10), "tau_P" = rexp(1,10), "beta" = rnorm(1,0,1), "gamma" =
851             rnorm(1,0,1), "delta" = rnorm(1,0,1), "theta0" = rnorm(1,0,1),
852             "effet_I"=rnorm(dim1,0,1),"effet_P"=rnorm(dim2,0,1), "inter"=inter0)
853         }
854         mod.Z010<-jags(inits=init.funZ010,model.file = "modelZ010_code.txt",data =
855         list("visit","ab_I","ab_P","dim1","dim2"),parameters.to.save =
856         c("mu","effet_I","effet_P","tau_I","tau_P","gamma","delta","beta","theta0","loglik"),n.chains = 1,
857         n.iter=1000000, n.burnin = 250000, n.thin = 250)
858         mod.Z010.mcmc<-as.mcmc(mod.Z010)
859         mZ010<-mod.Z010$BUGSoutput$sims.list
860         mZ010.deviance<-mZ010$deviance
861         mZ010.loglik<-mZ010$loglik
862         dimSEM<-dim(mZ010.loglik)[1]
863         list.mZ010<-sapply(1:dimSEM,function(x) matrix(mZ010.loglik[x,,],nrow=dim1*dim2))
864         list.tmZ010<-(t(list.mZ010))
865         mZ010.loo<-loo(list.tmZ010)
866         mZ010.loo
867         loo_file<-paste(dossier, "/", site, "_Z010_loo.txt", sep="")

```

```

868     write_values("mZ010", app=T, loo_file)
869     mZ010_loo_pointwise<-mZ010.loo$pointwise
870     mZ010_loo_pareto_k<-mZ010.loo$pareto_k
871     mZ010.loo$pareto_k<-NULL
872     mZ010.loo$pointwise<-NULL
873     write_values(as.matrix(mZ010.loo), app=T, loo_file)
874     save.image(paste(dossier, "/", site, "_Z010.RData", sep=""))
875 }
876 ### MODEL Z09
877 mZ09<-function(){
878     init.funZ09 <-function(){
879         list("tau_I" = rexp(1,10), "tau_P" = rexp(1,10), "beta" = rnorm(1,0,1), "delta" = rnorm(1,0,1),
880 "theta0" = rnorm(1,0,1), "epsilon" = rnorm(1,0,1),
881 "effet_I"=rnorm(dim1,0,1),"effet_P"=rnorm(dim2,0,1), "inter"=inter0)
882     }
883     mod.Z09<-jags(inits=init.funZ09,model.file = "modelZ09_code.txt",data =
884 list("cooc","visit","ab_P","dim1","dim2"),parameters.to.save =
885 c("mu","effet_I","effet_P","tau_I","tau_P","delta","beta","theta0","epsilon","loglik"),n.chains = 1,
886 n.iter=1000000, n.burnin = 250000, n.thin = 250)
887     mod.Z09.mcmc<-as.mcmc(mod.Z09)
888     mZ09<-mod.Z09$BUGSoutput$sims.list
889     mZ09.deviance<-mZ09$deviance
890     mZ09.loglik<-mZ09$loglik
891     dimSEM<-dim(mZ09.loglik)[1]
892     list.mZ09<-sapply(1:dimSEM,function(x) matrix(mZ09.loglik[x,,],nrow=dim1*dim2))
893     list.tmZ09<-(t(list.mZ09))

```



```

894     mZ09.loo<-loo(list.tmZ09)
895     mZ09.loo
896     loo_file<-paste(dossier, "/", site, "_Z09_loo.txt", sep="")
897     write_values("mZ09", app=T, loo_file)
898     mZ09_loo_pointwise<-mZ09.loo$pointwise
899     mZ09_loo_pareto_k<-mZ09.loo$pareto_k
900     mZ09.loo$pareto_k<-NULL
901     mZ09.loo$pointwise<-NULL
902     write_values(as.matrix(mZ09.loo), app=T, loo_file)
903     save.image(paste(dossier, "/", site, "_Z09.RData", sep=""))
904 }
905 ### MODEL Z08
906 mZ08<-function(){
907     init.funZ08 <-function(){
908         list("tau_I" = rexp(1,10), "tau_P" = rexp(1,10), "beta" = rnorm(1,0,1), "gamma" =
909         rnorm(1,0,1), "theta0" = rnorm(1,0,1), "epsilon" = rnorm(1,0,1),
910         "effet_I"=rnorm(dim1,0,1),"effet_P"=rnorm(dim2,0,1), "inter"=inter0)
911     }
912     mod.Z08<-jags(inits=init.funZ08,model.file = "modelZ08_code.txt",data =
913     list("cooc","visit","ab_I","dim1","dim2"),parameters.to.save =
914     c("mu","effet_I","effet_P","tau_I","tau_P","gamma","beta","theta0","epsilon","loglik"),n.chains = 1,
915     n.iter=1000000, n.burnin = 250000, n.thin = 250)
916     mod.Z08.mcmc<-as.mcmc(mod.Z08)
917     mZ08<-mod.Z08$BUGSoutput$sims.list
918     mZ08.deviance<-mZ08$deviance
919     mZ08.loglik<-mZ08$loglik

```

```

920     dimSEM<-dim(mZ08.loglik)[1]
921     list.mZ08<-sapply(1:dimSEM,function(x) matrix(mZ08.loglik[x,,],nrow=dim1*dim2))
922     list.tmZ08<-(t(list.mZ08))
923     mZ08.loo<-loo(list.tmZ08)
924     mZ08.loo
925     loo_file<-paste(dossier, "/", site, "_Z08_loo.txt", sep="")
926     write_values("mZ08", app=T, loo_file)
927     mZ08_loo_pointwise<-mZ08.loo$pointwise
928     mZ08_loo_pareto_k<-mZ08.loo$pareto_k
929     mZ08.loo$pareto_k<-NULL
930     mZ08.loo$pointwise<-NULL
931     write_values(as.matrix(mZ08.loo), app=T, loo_file)
932     save.image(paste(dossier, "/", site, "_Z08.RData", sep=""))
933 }
934 ### MODEL Z07
935 mZ07<-function(){
936     init.funZ07 <-function(){
937         list("tau_I" = rexp(1,10), "tau_P" = rexp(1,10), "alpha" = 0.1,"beta" = rnorm(1,0,1), "delta" =
938         rnorm(1,0,1), "theta0" = rnorm(1,0,1), "effet_I"=rnorm(dim1,0,1),"effet_P"=rnorm(dim2,0,1),
939         "inter"=inter0)
940     }
941     mod.Z07<-jags(inits=init.funZ07,model.file = "modelZ07_code.txt",data =
942     list("cooc","visit","ab_P","dim1","dim2"),parameters.to.save =
943     c("mu","effet_I","effet_P","tau_I","tau_P","alpha","delta","beta","theta0","loglik"),n.chains = 1,
944     n.iter=1000000, n.burnin = 250000, n.thin = 250)
945     mod.Z07.mcmc<-as.mcmc(mod.Z07)

```

```

946     mZ07<-mod.Z07$BUGSoutput$sims.list
947     mZ07.deviance<-mZ07$deviance
948     mZ07.loglik<-mZ07$loglik
949     dimSEM<-dim(mZ07.loglik)[1]
950     list.mZ07<-sapply(1:dimSEM,function(x) matrix(mZ07.loglik[x,,],nrow=dim1*dim2))
951     list.tmZ07<-(t(list.mZ07))
952     mZ07.loo<-loo(list.tmZ07)
953     mZ07.loo
954     loo_file<-paste(dossier, "/", site, "_Z07_loo.txt", sep="")
955     write_values("mZ07", app=T, loo_file)
956     mZ07_loo_pointwise<-mZ07.loo$pointwise
957     mZ07_loo_pareto_k<-mZ07.loo$pareto_k
958     mZ07.loo$pareto_k<-NULL
959     mZ07.loo$pointwise<-NULL
960     write_values(as.matrix(mZ07.loo), app=T, loo_file)
961     save.image(paste(dossier, "/", site, "_Z07.RData", sep=""))
962 }
963 ### MODEL Z06
964 mZ06<-function(){
965     init.funZ06 <-function(){
966         list("tau_I" = rexp(1,10), "tau_P" = rexp(1,10), "alpha" = 0.1,"beta" = rnorm(1,0,1), "gamma"
967 = rnorm(1,0,1), "theta0" = rnorm(1,0,1), "effet_I"=rnorm(dim1,0,1),"effet_P"=rnorm(dim2,0,1),
968 "inter"=inter0)
969     }
970     mod.Z06<<-jags(inits=init.funZ06,model.file = "modelZ06_code.txt",data =
971 list("cooc","visit","ab_I","dim1","dim2"),parameters.to.save =

```

```

972   c("mu","effet_I","effet_P","tau_I","tau_P","alpha","gamma","beta","theta0","loglik"),n.chains = 1,
973   n.iter=1000000, n.burnin = 250000, n.thin = 250)
974       mod.Z06.mcmc<-as.mcmc(mod.Z06)
975       mZ06<-mod.Z06$BUGSoutput$sims.list
976       mZ06.deviance<-mZ06$deviance
977       mZ06.loglik<-mZ06$loglik
978       dimSEM<-dim(mZ06.loglik)[1]
979       list.mZ06<-sapply(1:dimSEM,function(x) matrix(mZ06.loglik[x,,],nrow=dim1*dim2))
980       list.tmZ06<-(t(list.mZ06))
981       mZ06.loo<-loo(list.tmZ06)
982       mZ06.loo
983       loo_file<-paste(dossier, "/", site, "_Z06_loo.txt", sep="")
984       write_values("mZ06", app=T, loo_file)
985       mZ06_loo_pointwise<-mZ06.loo$pointwise
986       mZ06_loo_pareto_k<-mZ06.loo$pareto_k
987       mZ06.loo$pareto_k<-NULL
988       mZ06.loo$pointwise<-NULL
989       write_values(as.matrix(mZ06.loo), app=T, loo_file)
990       save.image(paste(dossier, "/", site, "_Z06.RData", sep=""))
991   }
992   ### MODEL Z05
993   mZ05<-function(){
994       init.funZ05 <-function(){
995           list("tau_I" = rexp(1,10), "tau_P" = rexp(1,10), "alpha" = 0.1,"beta" = rnorm(1,0,1), "theta0"
996   = rnorm(1,0,1), "epsilon" = rnorm(1,0,1), "effet_I"=rnorm(dim1,0,1),"effet_P"=rnorm(dim2,0,1),
997   "inter"=inter0)

```

```

998     }

999     mod.Z05<-jags(inits=init.funZ05,model.file = "modelZ05_code.txt",data =

1000 list("cooc","visit","dim1","dim2"),parameters.to.save =

1001 c("mu","effet_I","effet_P","tau_I","tau_P","alpha","beta","theta0","epsilon","loglik"),n.chains = 1,

1002 n.iter=1000000, n.burnin = 250000, n.thin = 250)

1003     mod.Z05.mcmc<-as.mcmc(mod.Z05)

1004     mZ05<-mod.Z05$BUGSoutput$sims.list

1005     mZ05.deviance<-mZ05$deviance

1006     mZ05.loglik<-mZ05$loglik

1007     dimSEM<-dim(mZ05.loglik)[1]

1008     list.mZ05<-sapply(1:dimSEM,function(x) matrix(mZ05.loglik[x,,],nrow=dim1*dim2))

1009     list.tmZ05<-(t(list.mZ05))

1010     mZ05.loo<-loo(list.tmZ05)

1011     mZ05.loo

1012     loo_file<-paste(dossier, "/", site, "_Z05_loo.txt", sep="")

1013     write_values("mZ05", app=T, loo_file)

1014     mZ05_loo_pointwise<-mZ05.loo$pointwise

1015     mZ05_loo_pareto_k<-mZ05.loo$pareto_k

1016     mZ05.loo$pareto_k<-NULL

1017     mZ05.loo$pointwise<-NULL

1018     write_values(as.matrix(mZ05.loo), app=T, loo_file)

1019     save.image(paste(dossier, "/", site, "_Z05.RData", sep=""))

1020 }

1021 ### MODEL Z04

1022 mZ04<-function(){

1023     init.funZ04 <-function(){

```

```

1024     list("tau_I" = rexp(1,10), "tau_P" = rexp(1,10), "beta" = rnorm(1,0,1), "gamma" =
1025     rnorm(1,0,1), "delta" = rnorm(1,0,1), "theta0" = rnorm(1,0,1), "epsilon" = rnorm(1,0,1),
1026     "effet_I"=rnorm(dim1,0,1),"effet_P"=rnorm(dim2,0,1), "inter"=inter0)
1027   }
1028   mod.Z04<-jags(inits=init.funZ04,model.file = "modelZ04_code.txt",data =
1029   list("cooc","visit","ab_I","ab_P","dim1","dim2"),parameters.to.save =
1030   c("mu","effet_I","effet_P","tau_I","tau_P","gamma","delta","beta","theta0","epsilon","loglik"),n.chai
1031   ns = 1, n.iter=1000000, n.burnin = 250000, n.thin = 250)
1032   mod.Z04.mcmc<-as.mcmc(mod.Z04)
1033   mZ04<-mod.Z04$BUGSoutput$sims.list
1034   mZ04.deviance<-mZ04$deviance
1035   mZ04.loglik<-mZ04$loglik
1036   dimSEM<-dim(mZ04.loglik)[1]
1037   list.mZ04<-sapply(1:dimSEM,function(x) matrix(mZ04.loglik[x,,],nrow=dim1*dim2))
1038   list.tmZ04<-(t(list.mZ04))
1039   mZ04.loo<-loo(list.tmZ04)
1040   mZ04.loo
1041   loo_file<-paste(dossier, "/", site, "_Z04_loo.txt", sep="")
1042   write_values("mZ04", app=T, loo_file)
1043   mZ04_loo_pointwise<-mZ04.loo$pointwise
1044   mZ04_loo_pareto_k<-mZ04.loo$pareto_k
1045   mZ04.loo$pareto_k<-NULL
1046   mZ04.loo$pointwise<-NULL
1047   write_values(as.matrix(mZ04.loo), app=T, loo_file)
1048   save.image(paste(dossier, "/", site, "_Z04.RData", sep=""))
1049 }

```

```

1050   ### MODEL Z03
1051   mZ03<-function(){
1052       init.funZ03 <-function(){
1053           list("tau_I" = rexp(1,10), "tau_P" = rexp(1,10), "alpha" = 0.1,"beta" = rnorm(1,0,1), "gamma"
1054   = rnorm(1,0,1), "theta0" = rnorm(1,0,1), "epsilon" = rnorm(1,0,1),
1055   "effet_I"=rnorm(dim1,0,1),"effet_P"=rnorm(dim2,0,1), "inter"=inter0)
1056       }
1057       mod.Z03<<-jags(inits=init.funZ03,model.file = "modelZ03_code.txt",data =
1058   list("cooc","visit","ab_I","dim1","dim2"),parameters.to.save =
1059   c("mu","effet_I","effet_P","tau_I","tau_P","alpha","gamma","beta","theta0","epsilon","loglik"),n.cha
1060   ins = 1, n.iter=1000000, n.burnin = 250000, n.thin = 250)
1061       mod.Z03.mcmc<-as.mcmc(mod.Z03)
1062       mZ03<-mod.Z03$BUGSoutput$sims.list
1063       mZ03.deviance<-mZ03$deviance
1064       mZ03.loglik<-mZ03$loglik
1065       dimSEM<-dim(mZ03.loglik)[1]
1066       list.mZ03<-sapply(1:dimSEM,function(x) matrix(mZ03.loglik[x,,],nrow=dim1*dim2))
1067       list.tmZ03<-(t(list.mZ03))
1068       mZ03.loo<-loo(list.tmZ03)
1069       mZ03.loo
1070       loo_file<-paste(dossier, "/", site, "_Z03_loo.txt", sep="")
1071       write_values("mZ03", app=T, loo_file)
1072       mZ03_loo_pointwise<-mZ03.loo$pointwise
1073       mZ03_loo_pareto_k<-mZ03.loo$pareto_k
1074       mZ03.loo$pareto_k<-NULL
1075       mZ03.loo$pointwise<-NULL

```

```

1076     write_values(as.matrix(mZ03.loo), app=T, loo_file)
1077     save.image(paste(dossier, "/", site, "_Z03.RData", sep=""))
1078 }
1079 ### MODEL Z02
1080 mZ02<-function(){
1081     init.funZ02 <-function(){
1082         list("tau_I" = rexp(1,10), "tau_P" = rexp(1,10), "alpha" = 0.1, "beta" = rnorm(1,0,1), "delta" =
1083         rnorm(1,0,1), "theta0" = rnorm(1,0,1), "epsilon" = rnorm(1,0,1),
1084         "effet_I"=rnorm(dim1,0,1),"effet_P"=rnorm(dim2,0,1), "inter"=inter0)
1085     }
1086     mod.Z02<-jags(inits=init.funZ02,model.file = "modelZ02_code.txt",data =
1087     list("cooc","visit","ab_P","dim1","dim2"),parameters.to.save =
1088     c("mu","effet_I","effet_P","tau_I","tau_P","alpha","delta","beta","theta0","epsilon","loglik"),n.chain
1089     s = 1, n.iter=1000000, n.burnin = 250000, n.thin = 250)
1090     mod.Z02.mcmc<-as.mcmc(mod.Z02)
1091     mZ02<-mod.Z02$BUGSoutput$sims.list
1092     mZ02.deviance<-mZ02$deviance
1093     mZ02.loglik<-mZ02$loglik
1094     dimSEM<-dim(mZ02.loglik)[1]
1095     list.mZ02<-sapply(1:dimSEM,function(x) matrix(mZ02.loglik[x,,],nrow=dim1*dim2))
1096     list.tmZ02<-(t(list.mZ02))
1097     mZ02.loo<-loo(list.tmZ02)
1098     mZ02.loo
1099     loo_file<-paste(dossier, "/", site, "_Z02_loo.txt", sep="")
1100     write_values("mZ02", app=T, loo_file)
1101     mZ02_loo_pointwise<-mZ02.loo$pointwise

```



```

1102     mZ02_loo_pareto_k<-mZ02.loo$pareto_k
1103     mZ02.loo$pareto_k<-NULL
1104     mZ02.loo$pointwise<-NULL
1105     write_values(as.matrix(mZ02.loo), app=T, loo_file)
1106     save.image(paste(dossier, "/", site, "_Z02.RData", sep=""))
1107 }
1108 ### MODEL Z01
1109 mZ01<-function(){
1110     init.funZ01 <-function(){
1111         list("tau_I" = rexp(1,10), "tau_P" = rexp(1,10), "alpha" = 0.1,"beta" = rnorm(1,0,1), "gamma"
1112 = rnorm(1,0,1), "delta" = rnorm(1,0,1), "theta0" = rnorm(1,0,1),
1113 "effet_I"=rnorm(dim1,0,1),"effet_P"=rnorm(dim2,0,1), "inter"=inter0)
1114     }
1115     mod.Z01<-jags(inits=init.funZ01,model.file = "modelZ01_code.txt",data =
1116 list("cooc","visit","ab_I","ab_P", "dim1", "dim2"),parameters.to.save =
1117 c("mu","effet_I","effet_P","tau_I","tau_P","alpha","gamma","delta","beta","theta0","loglik"),n.chain
1118 s = 1, n.iter=1000000, n.burnin = 250000, n.thin = 250)
1119     mod.Z01.mcmc<-as.mcmc(mod.Z01)
1120     mZ01<-mod.Z01$BUGSoutput$sims.list
1121     mZ01.deviance<-mZ01$deviance
1122     mZ01.loglik<-mZ01$loglik
1123     dimSEM<-dim(mZ01.loglik)[1]
1124     list.mZ01<-sapply(1:dimSEM,function(x) matrix(mZ01.loglik[x,,],nrow=dim1*dim2))
1125     list.tmZ01<-(t(list.mZ01))
1126     mZ01.loo<-loo(list.tmZ01)
1127     mZ01.loo

```

```

1128     loo_file<-paste(dossier, "/", site, "_Z01_loo.txt", sep="")
1129     write_values("mZ01", app=T, loo_file)
1130     mZ01_loo_pointwise<-mZ01.loo$pointwise
1131     mZ01_loo_pareto_k<-mZ01.loo$pareto_k
1132     mZ01.loo$pareto_k<-NULL
1133     mZ01.loo$pointwise<-NULL
1134     write_values(as.matrix(mZ01.loo), app=T, loo_file)
1135     save.image(paste(dossier, "/", site, "_Z01.RData", sep=""))
1136 }
1137 ### MODEL Z00
1138 mZ00<-function(){
1139     init.funZ00 <-function(){
1140         list("tau_I" = rexp(1,10), "tau_P" = rexp(1,10), "alpha" = 0.1,"beta" = rnorm(1,0,1), "gamma"
1141 = rnorm(1,0,1), "delta" = rnorm(1,0,1), "theta0" = rnorm(1,0,1), "epsilon" = rnorm(1,0,1),
1142 "effet_I"=rnorm(dim1,0,1),"effet_P"=rnorm(dim2,0,1), "inter"=inter0)
1143     }
1144     mod.Z00<-jags(inits=init.funZ00,model.file = "modelZ00_code.txt",data =
1145 list("cooc","visit","ab_I","ab_P","dim1","dim2"),parameters.to.save =
1146 c("mu","effet_I","effet_P","tau_I","tau_P","alpha","gamma","delta","beta","theta0","epsilon","loglik
1147 "),n.chains = 1, n.iter=1000000, n.burnin = 250000, n.thin = 250)
1148     mod.Z00.mcmc<-as.mcmc(mod.Z00)
1149     mZ00<-mod.Z00$BUGSoutput$sims.list
1150     mZ00.deviance<-mZ00$deviance
1151     mZ00.loglik<-mZ00$loglik
1152     dimSEM<-dim(mZ00.loglik)[1]
1153     list.mZ00<-sapply(1:dimSEM,function(x) matrix(mZ00.loglik[x,,],nrow=dim1*dim2))

```

```

1154     list.tmZ00<-(t(list.mZ00))
1155     mZ00.loo<-loo(list.tmZ00)
1156     mZ00.loo
1157     loo_file<-paste(dossier, "/", site, "_Z00_loo.txt", sep="")
1158     write_values("mZ00", app=T, loo_file)
1159     mZ00_loo_pointwise<-mZ00.loo$pointwise
1160     mZ00_loo_pareto_k<-mZ00.loo$pareto_k
1161     mZ00.loo$pareto_k<-NULL
1162     mZ00.loo$pointwise<-NULL
1163     write_values(as.matrix(mZ00.loo), app=T, loo_file)
1164     save.image(paste(dossier, "/", site, "_Z00.RData", sep=""))
1165 }
1166 ##### end model functions
1167 print("JOB DONE")
1168 #####
1169 ###   Network information (do not change)   ###
1170 #####
1171 #####BLOCK 3 – MODEL EXECUTION #####
1172 #launch_modele<-function(){
1173     ntw<-read.table(paste(dossier, "/", site, "_ntw.txt", sep=""),
1174     sep="\t",header=T,row.names=1)
1175     dim1<-dim(ntw)[1]
1176     dim2<-dim(ntw)[2]
1177     web<-as.matrix(ntw,dim1,dim2)
1178     inter0<-dget(paste(dossier, "/", site, "_web_i.txt", sep=""))
1179     cooc<-dget(paste(dossier, "/", site, "_co.txt", sep=""))

```

```

1180     visit<-read.table(paste(dossier, "/", site, "_ntw.txt", sep=""),sep="\t",header=T)
1181     visit<-as.matrix(visit)
1182     abundancel<-read.table(paste(dossier, "/", site, "_abl.txt", sep=""), sep="\t", header=T)
1183     ab_I <- log(abundancel[,2])
1184     abundanceP<-read.table(paste(dossier, "/", site, "_abP.txt", sep=""), sep="\t", header=T)
1185     ab_P <- log(abundanceP[,2])
1186     if(opt$modele == "all")
1187     {
1188         print("modele: all")
1189         for(i in 0:15)
1190         {
1191             print(paste("COMPUTING MODELE ", i, "\n", sep=""))
1192             mod<-eval(parse(text=paste("mZ0", i, sep="")))
1193             mod()
1194
1195         }
1196     }else{
1197         print(paste("modele: ", opt$modele), sep="")
1198         mod<-eval(parse(text=paste("m", opt$modele, sep="")))      #recupération de la
1199 fonction du modele
1200         mod()
1201     }
1202     ##### end model execution
1203     #launch_modele()
1204
1205     #####PARAMETER VALUES#####

```

```

1206 library(optparse)
1207 option_list = list(
1208     make_option(c("-d", "--dir"), type="character", default=NULL, help="model directory",
1209     metavar="character"),
1210     make_option(c("-s", "--site"), type="character", default=NULL, help="site name",
1211     metavar="character"))
1212 opt_parser = OptionParser(option_list=option_list);
1213 opt = parse_args(opt_parser);
1214 rdata<-list.files(opt$dir, pattern="*_Z015.RData")
1215 load(paste(opt$dir, "/", rdata, sep="")) #chargement du RData qui contient tous les modèles pour un
1216 site donné
1217 print(paste("RData ", rdata, " loaded", sep=""))
1218 for(mod in ls(pattern="mod.Z0*"))
1219 {
1220     print(paste("getting values from ", mod, sep=""))
1221     model<-eval(parse(text=mod))
1222     if(is.null(model$BUGSoutput$mean$alpha)){model$BUGSoutput$mean$alpha<-NA}
1223     if(is.null(model$BUGSoutput$mean$beta)){model$BUGSoutput$mean$beta<-NA}
1224     if(is.null(model$BUGSoutput$mean$delta)){model$BUGSoutput$mean$delta<-NA}
1225     if(is.null(model$BUGSoutput$mean$epsilon)){model$BUGSoutput$mean$epsilon<-NA}
1226     if(is.null(model$BUGSoutput$mean$gamma)){model$BUGSoutput$mean$gamma<-NA}
1227     val<-matrix(c(model$BUGSoutput$mean$alpha, model$BUGSoutput$mean$beta,
1228     model$BUGSoutput$mean$delta, model$BUGSoutput$mean$epsilon,
1229     model$BUGSoutput$mean$gamma), 1, 5, dimnames=list("values", c("alpha", "beta", "delta",
1230     "epsilon", "gamma")))

```

```
1231     write.table(val, file=paste(opt$dir, "/", opt$site, "_", mod, "_values.txt", sep=""), quote=F,  
1232     sep="\t", row.names=F, col.names=T)  
1233 }  
1234
```

1235 **Appendix S3: Modularity and latent block model analysis**

1236 We calculated the modularity of the network using the `cluster_leading_eigen` method for
1237 modularity optimization implemented in the `igraph` package (Csardi and Nepusz 2006, Newman
1238 2006). We then performed latent block models (LBM) using the `BM_poisson` method for
1239 quantitative network data implemented in the `blockmodels` package (Leger et al. 2015). Blocks
1240 are calculated separately for the two groups (insect and plant) based on the number of visits (*i.e.* a
1241 weighted network). The algorithm finds the best divisions of insects and plants through fitting one
1242 Poisson parameter in each block of the visit matrix, thus essentially maximizing the ICL (Integrated
1243 Completed Likelihood; Biernacki et al. 2000, Daudin et al. 2007).

```
1244  
1245 library(bipartite)  
1246 library(vegan)  
1247 library(igraph)  
1248 library(dummies)  
1249 library(blockmodels)  
1250 library(ade4)  
1251 library(fields)  
1252  
1253 #site data (ex: Bois de Fontaret, BFs)  
1254 BFs<-read.table("ntwBFs.txt",header=T,sep="\t")  
1255 webBFs <- as.matrix(BFs)  
1256 ##### Modularity analysis, binary data #####  
1257 BFs.graph.bin<-graph_from_incidence_matrix(webBFs,multiple=F) #binary  
1258 BFs.bin.cle<-cluster_leading_eigen(BFs.graph.bin)  
1259 BFs.bin.cle  
1260 #get phenology overlap matrix
```

```

1261 coBF<-dget("coBFs.txt")
1262 ##### LBM code: LBM analysis following Poisson #####
1263 bmi_BFs<-BM_poisson('LBM', webBFs)
1264 bmi_BFs$estimate()
1265 numi_BFs<-which.max(bmi_BFs$ICL)
1266 densi_BFs<-sum(webBFs)/(nrow(webBFs)*ncol(webBFs))
1267 probi_BFs<-bmi_BFs$model_parameters[[numi_BFs]]$lambda
1268 row.nb.gpi<-nrow(probi_BFs)
1269 col.nb.gpi<-ncol(probi_BFs)
1270 prob.rowi<-bmi_BFs$memberships[[numi_BFs]]$Z1
1271 hh.namei<-rownames(webBFs)
1272 mbrshp.hhi<-apply(prob.rowi,1,which.max)
1273 ls.freq.rowi<-rowSums(webBFs)
1274 res.hhi<-cbind.data.frame(hh.namei=hh.namei, mbrshp.hhi=mbrshp.hhi, freq.hhi=ls.freq.rowi)
1275 res.hh.ordi<-res.hhi[order(res.hhi$freq.hhi),]
1276 cpt=0
1277 for(k in 1: (nrow(res.hh.ordi)-1))
1278 {
1279   if (res.hh.ordi$mbrshp.hhi[k] !=res.hh.ordi$mbrshp.hhi[k+1]) cpt=cpt+1
1280 }
1281 nb.diff.hhi=cpt-(length(levels(as.factor(res.hh.ordi$mbrshp.hhi)))-1)
1282 #write tables
1283 write.table(res.hh.ordi,sep="\t",row.names=FALSE)
1284 prob.coli<-bmi_BFs$memberships[[numi_BFs]]$Z2
1285 sp.namei<-colnames(webBFs)
1286 mbrshp.spi<-apply(prob.coli,1,which.max)

```



```

1287 ls.freq.coli<-colSums(webBFs)
1288 res.spi<-cbind.data.frame(sp.namei=sp.namei, mbrshp.spi=mbrshp.spi, freq.spi=ls.freq.coli)
1289 res.sp.ordi<-res.spi[order(res.spi$freq.spi),]
1290 cpt=0
1291 for (k in 1: (nrow(res.sp.ordi)-1))
1292 {
1293   if(res.sp.ordi$mbrshp.spi[k] !=res.sp.ordi$mbrshp.spi[k+1]) cpt=cpt+1
1294 }
1295 nb.diff.spi=cpt-(length(levels(as.factor(res.sp.ordi$mbrshp.spi)))-1)
1296 res.sp.ord2i=res.spi[order(res.spi$mbrshp.spi),]
1297 write.table(res.sp.ordi,sep="\t",row.names=FALSE)
1298 write.table(probi_BFs,file="_prob_BFs",sep="\t",row.names=FALSE)
1299
1300 ##### Matrix organization #####
1301 par(mfrow=c(1,1))
1302 webBFs2<-webBFs
1303 webBFs[which(webBFs>1)]=1
1304 nb.row=nrow(webBFs)
1305 nb.col=ncol(webBFs)
1306 nds=webBFs
1307 nps=coBF
1308 res.prob=read.table("_prob_BFs",sep="\t",h=TRUE)
1309 ls.ord.col.prob=order(colSums(res.prob),decreasing=TRUE)
1310 ls.ord.row.prob=order(rowSums(res.prob),decreasing=TRUE)
1311 ls.ord.hhi=apply(res.hhi$mbrshp.hhi,function(x) which (x==ls.ord.row.prob))
1312 res.hh.ord2i=res.hhi[order(ls.ord.hhi),]

```

```

1313 row.nb.gpi=length(levels(as.factor(res.hhi$mbrshp.hhi)))
1314 res.hh.ord3i=NULL
1315 for (h in ls.ord.row.prob)
1316 {
1317   part=res.hh.ord2i[res.hh.ord2i$mbrshp.hhi==h,]
1318   part.ord=part[order(part$freq.hhi,decreasing=TRUE),]
1319   res.hh.ord3i=rbind.data.frame(res.hh.ord3i,part.ord)
1320 }
1321 ls.ord.sp=apply(res.spi$mbrshp.spi,function(x) which (x==ls.ord.col.prob))
1322 res.sp.ord2i=res.spi[order(ls.ord.sp),]
1323 col.nb.gb=length(levels(as.factor(res.spi$mbrshp.spi)))
1324 res.sp.ord3i=NULL
1325 for (h in ls.ord.col.prob)
1326 {
1327   part=res.sp.ord2i[res.sp.ord2i$mbrshp.spi==h,]
1328   part.ord=part[order(part$freq.spi,decreasing=TRUE),]
1329   res.sp.ord3i=rbind.data.frame(res.sp.ord3i,part.ord)
1330 }
1331 nds=nds[as.character(res.hh.ord3i$hh.namei),as.character(res.sp.ord3i$sp.namei)]
1332 nps=nps[as.character(res.hh.ord3i$hh.namei),as.character(res.sp.ord3i$sp.namei)]
1333 webBFs2=webBFs2[as.character(res.hh.ord3i$hh.namei),as.character(res.sp.ord3i$sp.namei)]
1334
1335 ##### Plot matrix with heatcolours and the number of visits #####
1336 visits<-matrix(webBFs2,nrow=dim(webBFs2)[1]*dim(webBFs2)[2],ncol=1)
1337 visits<-visits[which(visits>0)] #without the zeros
1338 coord.function<-function(x,nI,nP){

```

```

1339     c(((x-1)%%nl)+1,((x-1)%/%nl)+1)
1340 }
1341 func.plot.matrix<-function(x,y){
1342     indices<-which(x==1)
1343     min<-min(y)
1344     max<-max(y)
1345     yLabels<-rownames(x)
1346     xLabels<-colnames(x)
1347     title<-c("Bois de Fontaret")
1348     if(is.null(xLabels)){
1349         xLabels<-c(1:ncol(x))
1350     }
1351     if(is.null(yLabels)){
1352         yLabels<-c(1:nrow(x))
1353     }
1354     reverse<-nrow(x):1
1355     yLabels<-yLabels[reverse]
1356     y<-y[reverse,]
1357     image.plot(1:length(xLabels),1:length(yLabels),t(y),col=c("white",heat.colors(12)[12:1]), xlab="",
1358     ylab="",axes=FALSE,zlim=c(min,max))
1359     if(!is.null(title)){
1360         title(ylab="Insects", line=8, cex.lab=1)
1361         title(xlab="Plants", line=6, cex.lab=1.2)
1362         title("Bois de Fontaret")
1363     }
1364     axis(BELOW<-1,at=1:length(xLabels),labels=as.factor(as.character(xLabels)),las =2, cex.axis=0.6)

```

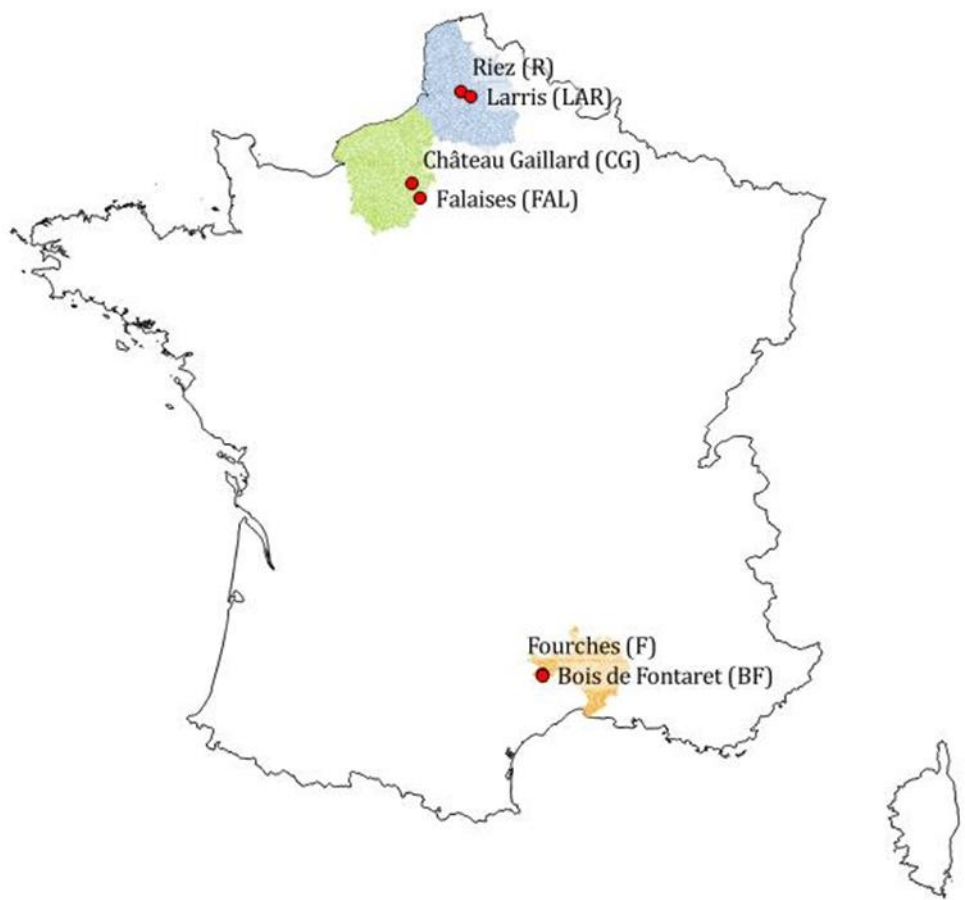
```

1365 axis(LEFT<-2,at=1:length(yLabels), labels=as.factor(as.character(yLabels)),las= 2,cex.axis=0.6)
1366 axis(BELOW<-1,at=1:length(xLabels),labels=rep("",length(xLabels)),las =2,cex.axis=0.6)
1367 axis(LEFT<-2,at=1:length(yLabels),labels=rep("",length(yLabels)),las=2,cex.axis<-0.6)
1368 coo<-t(rbind(sapply(indices,function(xx) coord.function(xx,nrow(x),ncol(x)))))
1369 text(coo[,2],nrow(webBFs)+1-coo[,1],labels=visits, cex=0.6)
1370 }
1371 func.plot.matrix(nds,nps)
1372 ##### Black lines to delimit blocks in the plot #####
1373 if (row.nb.gpi>1)
1374 {
1375   ls.class=as.numeric(as.data.frame(table(res.hh.ord2i$mbrshp.hhi))[ls.ord.row.prob,2])
1376   ls.cum=sum(ls.class)-cumsum(ls.class)
1377   abline(h=ls.cum+0.5,col="grey20", lwd=3)
1378 }
1379 if (col.nb.gpi>1)
1380 {
1381   ls.class=as.numeric(as.data.frame(table(res.sp.ord2i$mbrshp.spi))[ls.ord.col.prob,2])
1382   ls.cum=cumsum(ls.class)
1383   abline(v=ls.cum+0.5,col="grey20", lwd=3)
1384 }

```

1385

Figures and Tables



1386

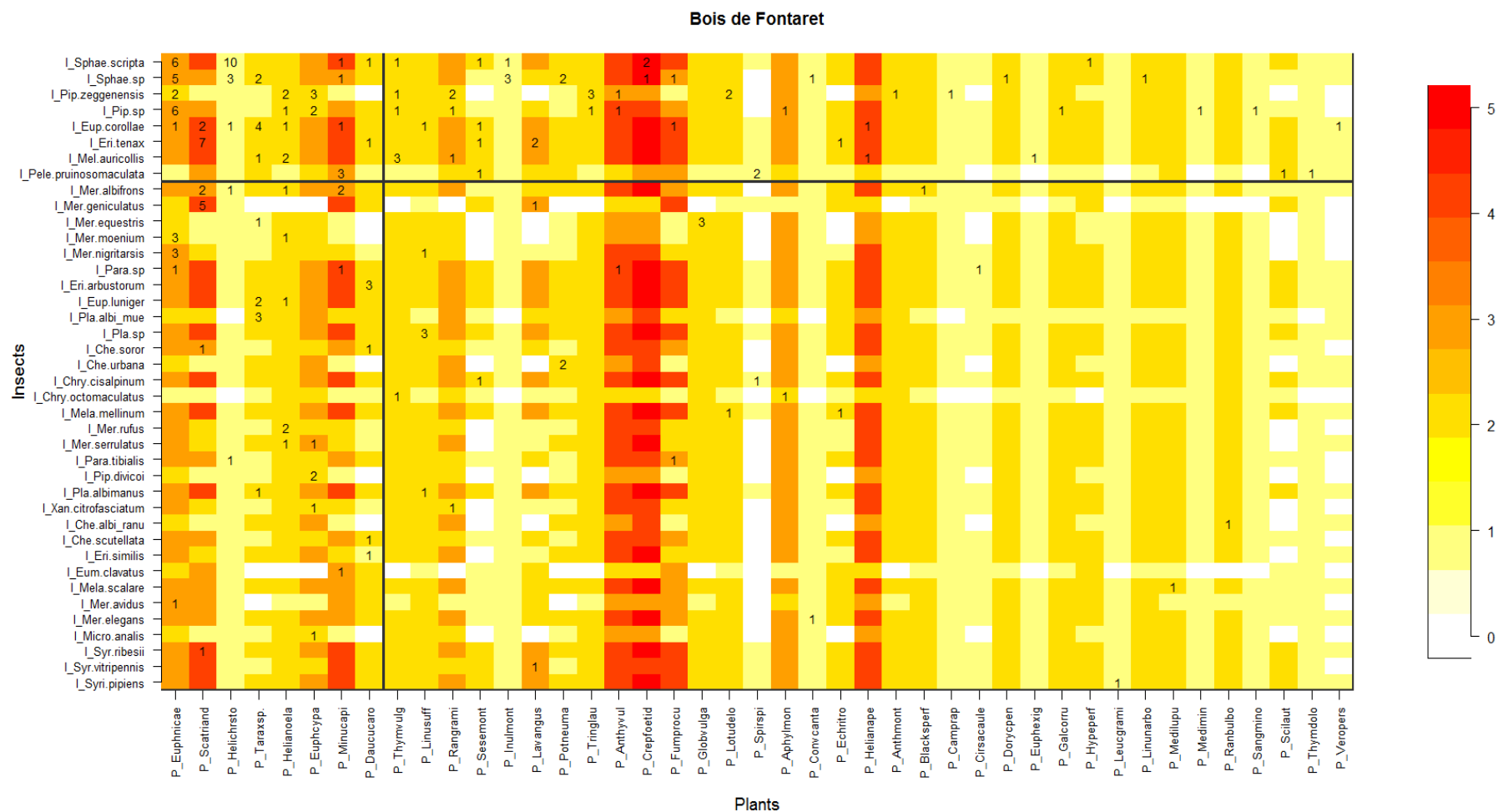
1387

1388

1389

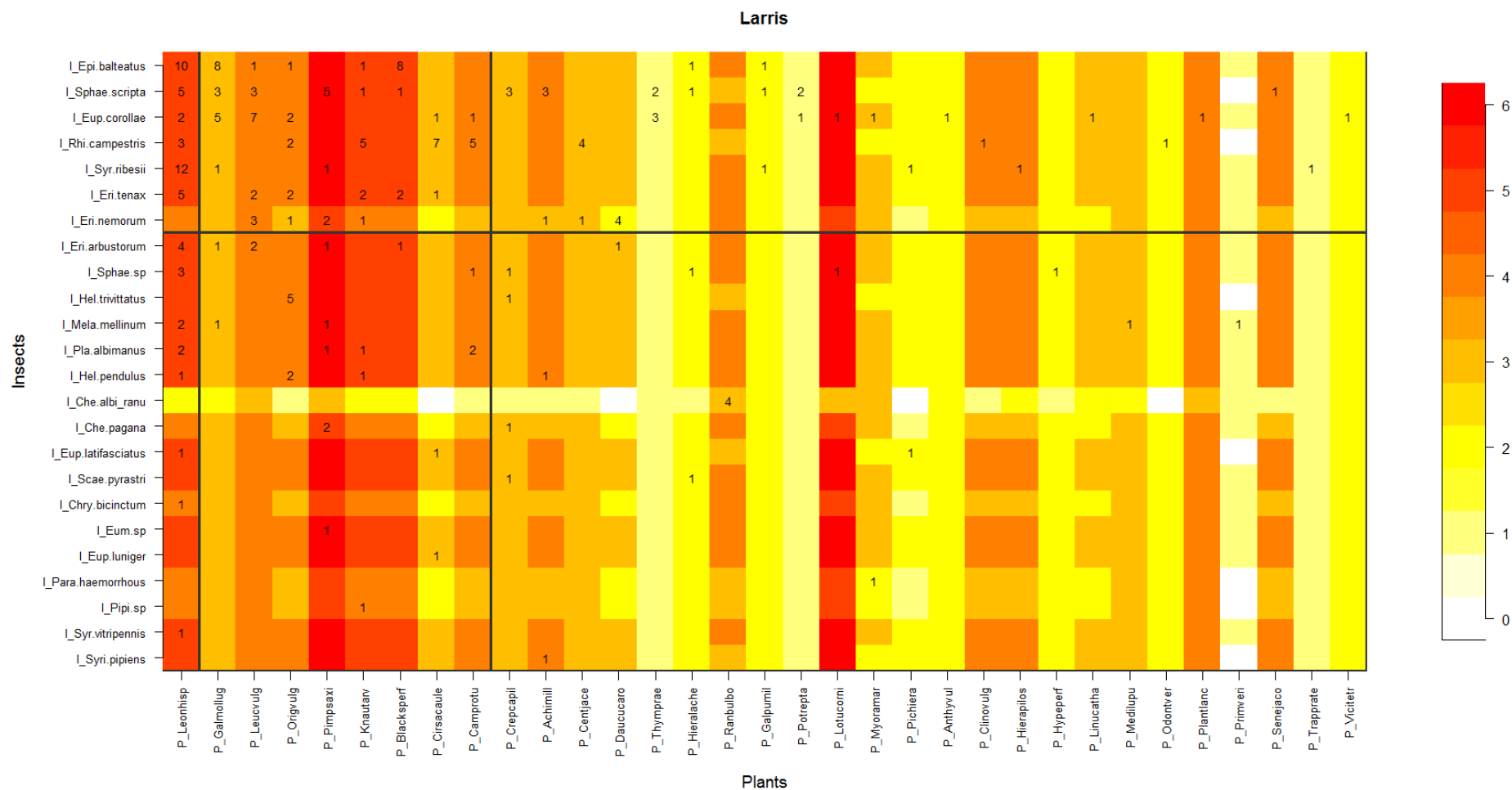
1390

Figure S1. Site location in France: in blue the French départements Pas-de-Calais and Somme (Hauts-de-France region), in green the départements Eure and Seine Maritime (Normandie region), in orange the département Gard (Occitanie region). The six sites correspond to the red dots.



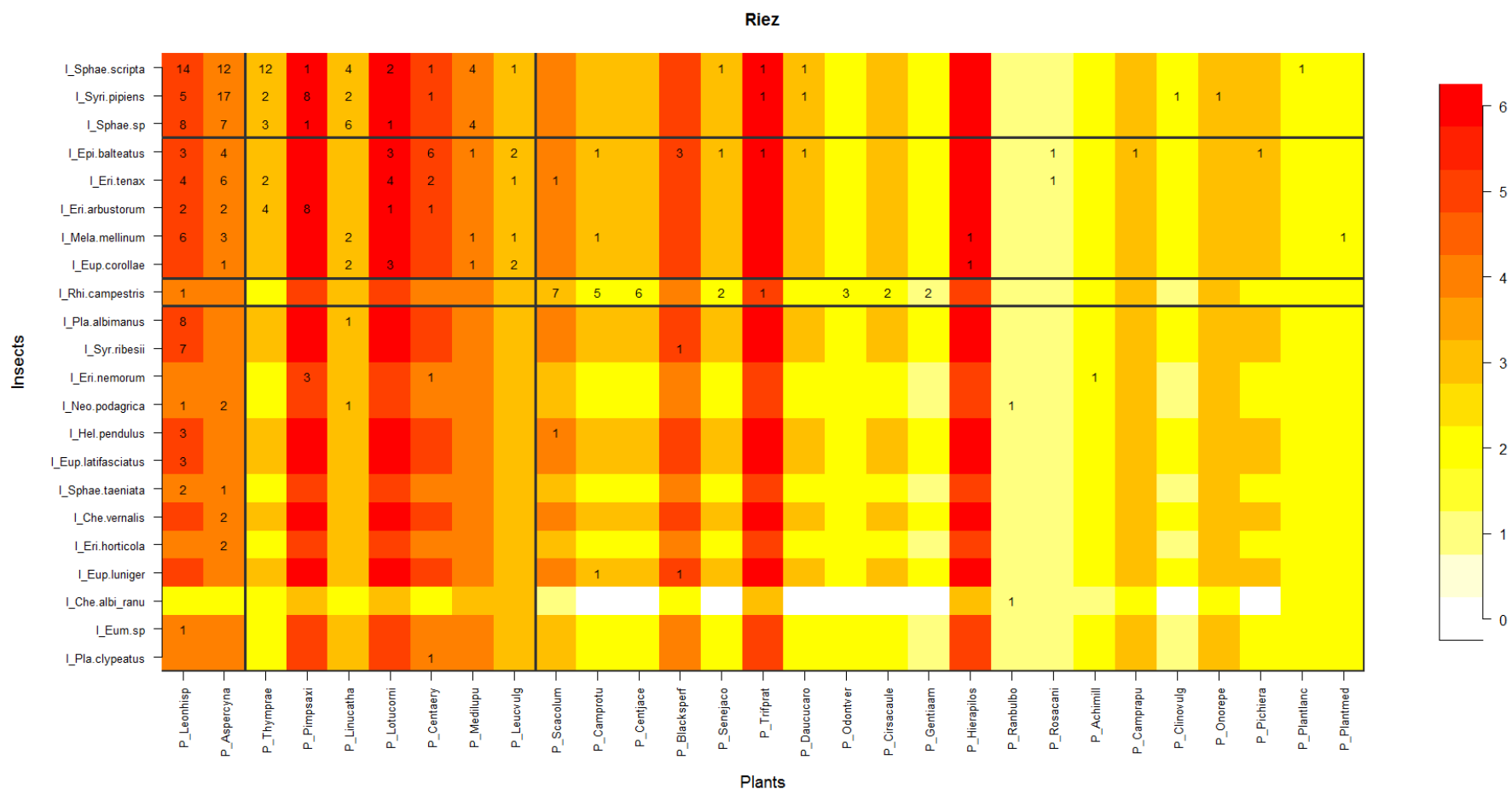
1391

1392 Figure S2. Block clustering provided by LBM in the site of Bois de Fontaret (BF, Occitanie), overlaid on a heatmap of species phenology overlap. Insect species
 1393 are displayed in rows and plant species in columns, following their degree (number of partners). The blocks of insects and the blocks of plants are separated
 1394 by solid black lines. Colours correspond to the number of months that are shared by each pair of plant and insect species (PO, phenology overlap), with higher
 1395 PO corresponding to darker colours. Numbers are the number of visits observed in the field for a given plant-insect pair.



1401

1402 Figure S4. Block clustering provided by LBM in the site of Larris (LAR, Hauts-de-France), overlaid on a heatmap of species phenology overlap. Insect species
 1403 are displayed in rows and plant species in columns, following their degree (number of partners). The blocks of insects and the blocks of plants are separated
 1404 by solid black lines. Colours correspond to the number of months that are shared by each pair of plant and insect species (PO, phenology overlap), with higher
 1405 PO corresponding to darker colours. Numbers are the number of visits observed in the field for a given plant-insect pair.



1406

1407 Figure S5. Block clustering provided by LBM in the site of Riez (R, Hauts-de-France), overlaid on a heatmap of species phenology overlap. Insect species are
 1408 displayed in rows and plant species in columns, following their degree (number of partners). The blocks of insects and the blocks of plants are separated by
 1409 solid black lines. Colours correspond to the number of months that are shared by each pair of plant and insect species (PO, phenology overlap), with higher
 1410 PO corresponding to darker colours. Numbers are the number of visits observed in the field for a given plant-insect pair.

1411 Table S1. Table of transformed plant abundances. The first column shows the Braun-Blanquet
 1412 coefficients of, the second column, their percentages, and the third column, the transformed
 1413 abundances used as the plant abundances in the model.

Coefficient Braun-Blanquet	Abundance percentage interval	Abundance percentage
<i>i</i>	1 individual	0.1%
+	< 1 %	0.5%
1	1-10 %	5%
2	10-25 %	15%
3	25-50 %	35%
4	50-75 %	65%
5	75-100 %	85%

1414